

# Sharp bounds of constants in Poincaré-type inequalities for simplicial domains

S. Matculevich and S. Repin

Department of Mathematical Information Technology, University of Jyväskylä  
 FIN-40100 Jyväskylä, FINLAND  
 e-mails: svetlana.v.matculevich@jyu.fi, sergey.repin@jyu.fi

St. Petersburg Dept. of V.A. Steklov Institute of Mathematics of RAS  
 St. Petersburg, Russia

October 10, 2018

## Abstract

The paper is concerned with sharp estimates of constants in classical Poincaré inequalities and Poincaré-type inequalities for functions having zero mean value in a simplicial domain or on a part of its boundary. These estimates are important for quantitative analysis of problems generated by differential equations where numerical approximations are typically constructed with the help of simplicial meshes. We suggest easily computable relations that provide sharp bounds of the respective constants and compare these results with analytical estimates (if they are known). In the last section, we present an example that shows possible applications of the results and derive a computable majorant of the difference between the exact solution of a boundary value problem and an arbitrary finite dimensional approximation computed on a simplicial mesh, which uses above mentioned constants.

## 1 Introduction

Let  $T$  be an open bounded connected domain in  $\mathbb{R}^d$  ( $d \geq 2$ ) with Lipschitz boundary  $\partial T$ . It is well known that the Poincaré inequality ([29, 30])

$$\|w\|_T \leq C_T^P \|\nabla w\|_T \quad (1)$$

holds for any

$$w \in \tilde{H}^1(T) := \left\{ w \in H^1(T) \mid \{w\}_T = 0 \right\},$$

where  $\|w\|_T$  denotes the norm in  $L^2(T)$ ,  $\{w\}_T := \frac{1}{|T|} \int_T w \, dx$  is the mean value of  $w$ , and  $|T|$  is the Lebesgue measure of  $T$ . The constant  $C_T^P$  depends only on  $T$  and  $d$ .

Poincaré-type inequalities also hold for

$$w \in \tilde{H}^1(T, \Gamma) := \left\{ w \in H^1(T) \mid \{w\}_\Gamma = 0 \right\},$$

where  $\Gamma$  is a measurable part of  $\partial T$  such that  $\text{meas}_{d-1} \Gamma > 0$  (in particular,  $\Gamma$  may coincide with the whole boundary). For any  $w \in \tilde{H}^1(T, \Gamma)$ , we have two inequalities similar to (1). The first one

$$\|w\|_T \leq C_\Gamma^P \|\nabla w\|_T \quad (2)$$

is another form of the Poincaré inequality (1), which is stated for a different set of functions and contains a different constant, i.e.  $C_\Gamma^P \leq C_T^P$ . The constant  $C_\Gamma^P$  is associated with the minimal positive eigenvalue of the problem

$$-\Delta u = \lambda u \text{ in } T; \quad \partial_n u = \lambda \{u\} \text{ on } \Gamma; \quad \partial_n u = 0 \text{ on } \partial T \setminus \Gamma, \quad \forall u \in H^1(T, \Gamma). \quad (3)$$

The second inequality

$$\|w\|_\Gamma \leq C_\Gamma^{\text{Tr}} \|\nabla w\|_T \quad (4)$$

estimates the trace of  $w \in \tilde{H}^1(T, \Gamma)$  on  $\Gamma$ . It is associated with the minimal nonzero eigenvalue of the problem

$$-\Delta u = 0 \text{ in } T; \quad \partial_n u = \lambda u \text{ on } \Gamma; \quad \partial_n u = 0 \text{ on } \partial T \setminus \Gamma, \quad \forall u \in H^1(T, \Gamma). \quad (5)$$

The problem (5) is a special case of the Steklov problem with spectral parameter appearing in the boundary condition. It is called the sloshing problem, which describes the oscillations of fluid in a container. The extensive study of the properties of sloshing eigenvalues and eigenfunctions can be found in [9, 2, 15, 16, 17] and references therein. The question on the spectrum of the operator corresponding to the latter problem also have gained interest from the viewpoint of spectral geometry (see [11]).

Poincaré-type inequalities are often used in analysis of nonconforming approximations (e.g., discontinuous Galerkin or mortar methods), domain decomposition methods (see, e.g., [14, 8] and [34]), analysis of problems described in terms of vector valued functions (see, e.g., [10, 26]), a posteriori estimates, and other applications related to quantitative analysis of partial differential equations. In [13, 20], the analysis of error constants for piecewise constant and linear interpolations over triangular finite elements can be found. Paper [4] introduces fully computable two-sided bounds on the eigenvalues of the Laplace operator based on the approximation of the corresponding eigenfunction in the nonconforming Crouzeix-Raviart FE space. Therefore, exact values of respective constants (or sharp and guaranteed bounds of them) are interesting from both analytical and computational points of view.

It is known that for convex domains  $C_T^P \leq \frac{\text{diam}(T)}{\pi}$  (see [27]). However, for triangles this estimate was improved in [19], i.e.,  $C_T^P \leq \frac{\text{diam}(T)}{j_{1,1}}$ , where  $j_{1,1} \approx 3.8317$  is the smallest positive root of the Bessel function  $J_1$ . Moreover, for isosceles triangles it was shown that

$$C_T^P \leq \overline{C}_T^{P, \Delta} := \text{diam}(T) \cdot \begin{cases} \frac{1}{j_{1,1}} & \alpha \in (0, \frac{\pi}{3}], \\ \min \left\{ \frac{1}{j_{1,1}}, \frac{1}{j_{0,1}} (2(\pi - \alpha) \tan(\alpha/2))^{-1/2} \right\} & \alpha \in (\frac{\pi}{3}, \frac{\pi}{2}], \\ \frac{1}{j_{0,1}} (2(\pi - \alpha) \tan(\alpha/2))^{-1/2} & \alpha \in (\frac{\pi}{2}, \pi). \end{cases} \quad (6)$$

Here,  $j_{0,1} \approx 2.4048$  and  $j_{1,1} \approx 3.8317$  are the smallest positive roots of the Bessel functions  $J_0$  and  $J_1$ , respectively. A lower bound of  $C_T^P$  for convex domains was derived in [6]. It was shown that

$$C_T^P \geq \frac{\text{diam}(T)}{2j_{0,1}}. \quad (7)$$

This estimate compliments the upper bound presented by the Payne–Weinberger estimate, and according to [1], is known to be the best lower bound for general domains with diameter scaling among all known so far. However, for triangles work [18] provides lower bound

$$C_T^P \geq \frac{P}{4\pi}, \quad (8)$$

which improves (7) for some cases. Here,  $P$  is perimeter of  $T$ .

Exact values of  $C_\Gamma^P$  and  $C_\Gamma^{\text{Tr}}$  were derived in [25] for parallelepipeds, rectangles, and right triangles. Below, we present a concise summary of these results related to the case  $d = 2$ :

1. If  $T := \text{conv}\{(0, 0), (0, h), (h, 0)\}$ , and  $\Gamma := \{x_1 \in [0, h], x_2 = 0\}$  (i.e.,  $\Gamma$  coincides with one of the legs of the isosceles right triangle), then

$$C_\Gamma^P = \frac{h}{\zeta_0}, \quad \text{and} \quad C_\Gamma^{\text{Tr}} = \left( \frac{h}{\zeta_0 \tanh(\hat{\zeta}_0)} \right)^{1/2}, \quad (9)$$

where  $\zeta_0$  and  $\hat{\zeta}_0$  are unique roots in  $(0, \pi)$  of the equations

$$z \cot(z) + 1 = 0 \quad \text{and} \quad \tan(z) + \tanh(z) = 0, \quad (10)$$

respectively.

2. If  $T := \text{conv}\{(0, 0), (0, h), (\frac{h}{2}, \frac{h}{2})\}$  and  $\Gamma$  coincides with the hypotenuse of the isosceles right triangle, then

$$C_\Gamma^P = \frac{h}{2\zeta_0}, \quad \text{and} \quad C_\Gamma^{\text{Tr}} = \left( \frac{h}{2} \right)^{1/2}.$$

It is worth noting that values of constant  $C_\Gamma^{\text{Tr}}$  on the right isosceles triangle follow from the exact solutions of Steklov problem on the square. This specific case was mentioned in the work [11].

Exact value of constants in classical Poincaré inequality on equilateral triangle  $T_{\pi/3} := \text{conv}\{(0, 0), (1, 0), (\frac{1}{2}, \frac{\sqrt{3}}{2})\}$  is derived in [28], i.e.,  $C_{\Gamma, \pi/2, \pi/3}^P = \frac{3}{4\pi}$ . Constants for the right isosceles triangles with legs  $\frac{\sqrt{2}}{2}$  and 1, which are defined correspondingly as  $T_{\pi/4} := \text{conv}\{(0, 0), (1, 0), (\frac{1}{2}, \frac{1}{2})\}$  and  $T_{\pi/2} := \text{conv}\{(0, 0), (1, 0), (0, 1)\}$ , are  $C_{\hat{T}, \pi/4}^P = \frac{1}{\sqrt{2}\pi}$

and  $C_{\hat{T}, \pi/2}^P = \frac{1}{\pi}$ , respectively. The latter one can be found from [12] and [13]. Explicit formulas of the same constants for some three-dimensional domains can be found in papers [3] and [12].

Above mentioned results form a basis for deriving sharp bounds of the constants  $C_\Gamma^P$ ,  $C_\Gamma^{\text{Tr}}$ , and  $C_T^P$  for arbitrary non-degenerate triangles and tetrahedrons, which are typical objects in various discretization methods. In Section 2, we deduce guaranteed and easily computable bounds of  $C_\Gamma^P$ ,  $C_\Gamma^{\text{Tr}}$ , and  $C_T^P$  for triangular domains. The efficiency of these bounds is tested in Section 3, where  $C_\Gamma^P$ ,  $C_\Gamma^{\text{Tr}}$  are compared with lower bounds computed numerically by solving generalized eigenvalue problem generated by Rayleigh quotients discretized over sufficiently representative sets of trial functions. In the same section, we make a similar comparison of numerical lower bounds related to the constant  $C_T^P$  with obtained upper bounds and existing estimates known from works [18, 19] and [6]. Lower bounds of the constants presented in Section 3 have been computed by two independent codes. The first code is based on MATLAB Symbolic Math Toolbox [33], and the second one uses The FEniCS Project [21]. Section 4 is devoted to tetrahedrons. We combine numerical and theoretical estimates in order to derive two sided bounds of the constants. For convinience of the reader, we collect all the figures in Appendix 6. Finally, in Section 5 we present an example that shows one possible application of the estimates considered in previous sections. Here, the constants are used in order to deduce a guaranteed and fully computable upper bound of the distance between the exact solution of an elliptic boundary value problem and an arbitrary function (approximation) in the respective energy space.

## 2 Majorants of $C_\Gamma^P$ and $C_\Gamma^{\text{Tr}}$ for triangular domains

We set

$$T = \text{conv}\{(0, 0), (h, 0), (h\rho \cos \alpha, h\rho \sin \alpha)\} \quad \text{and} \quad \Gamma := \{x_1 \in [0, h]; x_2 = 0\}, \quad (11)$$

where  $\rho > 0$ ,  $h > 0$ , and  $\alpha \in (0, \pi)$  are geometrical parameters that fully define a triangle  $T$  (see Fig. 1). Lemma below is based on analysis of the mapping from the reference triangles to (11) using well known transformation of the integrals (see, e.g., [7]). Easily computable bounds of  $C_\Gamma^P$  and  $C_\Gamma^{\text{Tr}}$  are presented below.

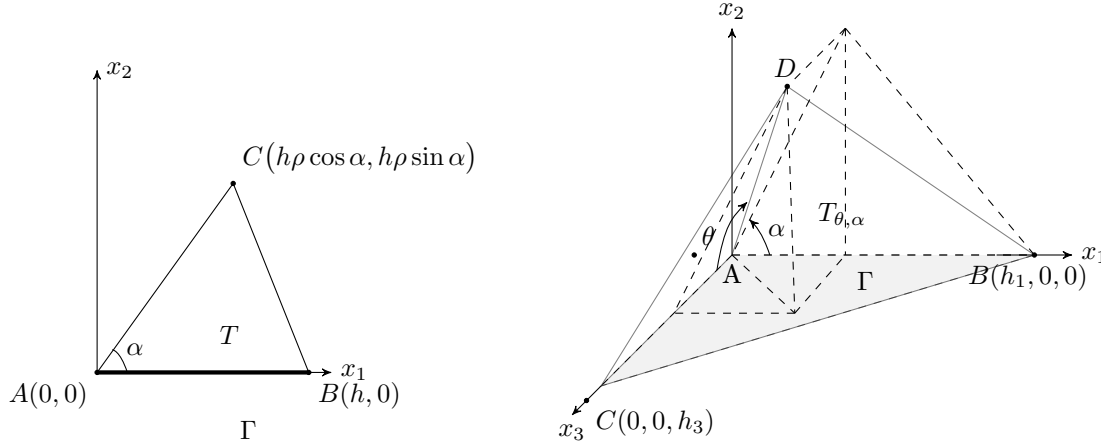


Figure 1: Simplex in  $\mathbb{R}^2$ .

Figure 2: Simplex in  $\mathbb{R}^3$ .

**Lemma 1** For any  $w \in \tilde{H}^1(T, \Gamma)$ , the estimates

$$\|w\|_T \leq C_\Gamma^P h \|\nabla w\|_T \quad \text{and} \quad \|w\|_\Gamma \leq C_\Gamma^{\text{Tr}} h^{1/2} \|\nabla w\|_T \quad (12)$$

hold with

$$C_\Gamma^P \leq \bar{C}_\Gamma^P = \min \left\{ c_{\pi/2}^P C_{\hat{\Gamma}, \pi/2}^P, c_{\pi/4}^P C_{\hat{\Gamma}, \pi/4}^P \right\} \quad \text{and} \quad C_\Gamma^{\text{Tr}} \leq \bar{C}_\Gamma^{\text{Tr}} = \min \left\{ c_{\pi/2}^{\text{Tr}} C_{\hat{\Gamma}, \pi/2}^{\text{Tr}}, c_{\pi/4}^{\text{Tr}} C_{\hat{\Gamma}, \pi/4}^{\text{Tr}} \right\},$$

respectively. Here,

$$c_{\pi/2}^P = \mu_{\pi/2}^{1/2}, \quad c_{\pi/2}^{\text{Tr}} = (\rho \sin \alpha)^{-1/2} c_{\pi/2}^P, \quad c_{\pi/4}^P = \mu_{\pi/4}^{1/2}, \quad c_{\pi/4}^{\text{Tr}} = (2\rho \sin \alpha)^{-1/2} c_{\pi/4}^P,$$

where

$$\mu_{\pi/2}(\rho, \alpha) = \frac{1}{2} \left( 1 + \rho^2 + (1 + \rho^4 + 2\rho^2 \cos 2\alpha)^{1/2} \right), \quad (13)$$

$$\mu_{\pi/4}(\rho, \alpha) = 2\rho^2 - 2\rho \cos \alpha + 1 + ((2\rho^2 + 1)(2\rho^2 + 1 - 4\rho \cos \alpha + 4\rho^2 \cos 2\alpha))^{1/2}, \quad (14)$$

and  $C_{\widehat{\Gamma}, \pi/2}^{\text{P}} \approx 0.49291$ ,  $C_{\widehat{\Gamma}, \pi/2}^{\text{Tr}} \approx 0.65602$  and  $C_{\widehat{\Gamma}, \pi/4}^{\text{P}} \approx 0.24646$ ,  $C_{\widehat{\Gamma}, \pi/4}^{\text{Tr}} \approx 0.70711$ .

**Proof:** Consider a linear mapping  $\mathcal{F}_{\pi/2} : \widehat{T}_{\pi/2} \rightarrow T$

$$x = \mathcal{F}_{\pi/2}(\widehat{x}) = B_{\pi/2} \widehat{x}, \quad \text{where} \quad B_{\pi/2} = \begin{pmatrix} h & \rho h \cos \alpha \\ 0 & \rho h \sin \alpha \end{pmatrix}, \quad \det B_{\pi/2} = \rho h^2 \sin \alpha.$$

For any  $\widehat{w} \in \widetilde{H}^1(\widehat{T}_{\pi/2}, \widehat{\Gamma})$ , we have the estimate

$$\|\widehat{w}\|_{\widehat{T}_{\pi/2}} \leq C_{\widehat{\Gamma}, \pi/2}^{\text{P}} \|\nabla \widehat{w}\|_{\widehat{T}_{\pi/2}}, \quad (15)$$

where  $C_{\widehat{\Gamma}, \pi/2}^{\text{P}}$  is the constant associated with the basic simplex

$$T_{\pi/2} := \text{conv}\{(0, 0), (1, 0), (0, 1)\}. \quad (16)$$

Note that

$$\|\widehat{w}\|_{\widehat{T}_{\pi/2}}^2 = \frac{1}{\rho h^2 \sin \alpha} \|w\|_T^2, \quad (17)$$

and

$$\|\nabla \widehat{w}\|_{\widehat{T}_{\pi/2}}^2 \leq \frac{1}{\rho h^2 \sin \alpha} \int_T A_{\pi/2}(h, \rho, \alpha) \nabla w \cdot \nabla w \, dx, \quad (18)$$

where

$$A_{\pi/2}(h, \rho, \alpha) = h^2 \begin{pmatrix} 1 + \rho^2 \cos^2 \alpha & \rho^2 \sin \alpha \cos \alpha \\ \rho^2 \sin \alpha \cos \alpha & \rho^2 \sin^2 \alpha \end{pmatrix}.$$

It is not difficult to see that

$$\lambda_{\max}(A_{\pi/2}) = h^2 \mu_{\pi/2}(\rho, \alpha), \quad \mu_{\pi/2}(\rho, \alpha) = \frac{1}{2} \left( 1 + \rho^2 + (1 + \rho^4 + 2 \cos 2\alpha \rho^2)^{1/2} \right),$$

where  $\mu_{\pi/2}(\rho, \alpha)$  is defined in (13). We use (15), (17), and (18), and obtain

$$\|w\|_T \leq c_{\pi/2}^{\text{P}} C_{\widehat{\Gamma}, \pi/2}^{\text{P}} h \|\nabla w\|_T, \quad c_{\pi/2}^{\text{P}}(\rho, \alpha) = \mu_{\pi/2}^{1/2}(\rho, \alpha). \quad (19)$$

Next, in view of (4), for any  $\widehat{w} \in \widetilde{H}^1(\widehat{T}_{\pi/2}, \widehat{\Gamma})$  we have

$$\|\widehat{w}\|_{\widehat{\Gamma}} \leq C_{\widehat{\Gamma}, \pi/2}^{\text{Tr}} \|\nabla \widehat{w}\|_{\widehat{T}_{\pi/2}},$$

where  $C_{\widehat{\Gamma}, \pi/2}^{\text{Tr}}$  is the constant associated with the reference simplex

$$\widehat{T}_{\pi/4} := \text{conv}\{(0, 0), (1, 0), (\frac{1}{2}, \frac{1}{2})\}. \quad (20)$$

Since

$$\|\widehat{w}\|_{\widehat{\Gamma}}^2 = \frac{1}{h} \|w\|_{\Gamma}^2,$$

we obtain

$$\|w\|_{\Gamma} \leq c_{\pi/2}^{\text{Tr}} C_{\widehat{\Gamma}, \pi/2}^{\text{Tr}} h^{1/2} \|\nabla w\|_T, \quad c_{\pi/2}^{\text{Tr}}(\rho, \alpha) = \left( \frac{\mu_{\pi/2}(\rho, \alpha)}{\rho \sin \alpha} \right)^{1/2}. \quad (21)$$

The mapping

$$x = \mathcal{F}_{\pi/4}(\widehat{x}) = B_{\pi/4} \widehat{x}, \quad \text{where} \quad B_{\pi/4} = \begin{pmatrix} h & 2\rho h \cos \alpha - h \\ 0 & 2\rho h \sin \alpha \end{pmatrix} \quad \text{and} \quad \det B_{\pi/4} = 2\rho h^2 \sin \alpha > 0,$$

yields another pair of estimates for the functions in  $\widetilde{H}^1(T, \Gamma)$ :

$$\|w\|_T \leq c_{\pi/4}^{\text{P}} C_{\widehat{\Gamma}, \pi/4}^{\text{P}} h \|\nabla w\|_T, \quad c_{\pi/4}^{\text{P}}(\rho, \alpha) = \mu_{\pi/4}^{1/2}(\rho, \alpha), \quad (22)$$

and

$$\|w\|_{\Gamma} \leq c_{\pi/4}^{\text{Tr}} C_{\widehat{\Gamma}, \pi/4}^{\text{Tr}} h^{1/2} \|\nabla w\|_T, \quad c_{\pi/4}^{\text{Tr}}(\rho, \alpha) = \left( \frac{\mu_{\pi/4}(\rho, \alpha)}{2\rho \sin \alpha} \right)^{1/2}, \quad (23)$$

where  $\mu_{\pi/4}(\rho, \alpha)$  is defined in (14). Now, (12) follows from (19), (21), (22), and (23).  $\square$

**Remark 1** The selection of  $\Gamma$  and  $\alpha$  in  $T$  depends on the finite element implementation, i.e., we select  $\Gamma$  out three edges of  $T$  such that it satisfies the condition  $\{w\}_\Gamma = 0$ . According to the results of numerical experiments, to provide optimal values of  $C_\Gamma^P$ ,  $\Gamma$  must coincide with with longest side of  $T$ , and between two adjacent angles we select minimum one to be  $\alpha$ . For the constant  $C_\Gamma^{\text{Tr}}$ , minimum values are attained for  $\alpha$  lying in the interval  $(\frac{\pi}{3}, \frac{2\pi}{3})$  (see Section 3).

**Remark 2** Let us show that obtained  $w$  belongs to the correct space. Assume that  $w \in \tilde{H}^1(\hat{T}, \hat{\Gamma})$  and consider mean value of  $w$  after the transformation. We note that

$$\{w\}_\Gamma := \int_\Gamma w(x) ds = h \int_{\hat{\Gamma}} w(x(\hat{x})) d\hat{s} = h \int_{\hat{\Gamma}} \hat{w} d\hat{s} = 0.$$

Therefore, the mean value of the function on the boundary remains zero and indeed  $w \in \tilde{H}^1(T, \Gamma)$ .

Analogously to Lemma 1, one can obtain the upper bound of the constant in (1). For that we consider three reference triangle  $T_{\pi/2}$ ,  $T_{\pi/4}$  (defined in (16) and (20)), and  $T_{\pi/3} := \text{conv}\{(0, 0), (1, 0), (\frac{1}{2}, \frac{\sqrt{3}}{2})\}$ .

**Lemma 2** For any  $w \in \tilde{H}^1(T)$ , the estimate of the constant in

$$\|w\|_T \leq C_\Omega^P h \|\nabla w\|_T \quad (24)$$

has the form

$$C_\Gamma^P \leq \bar{C}_T^P = \min \left\{ \bar{c}_{\pi/4} C_{\hat{T}, \pi/4}^P, \bar{c}_{\pi/3} C_{\hat{T}, \pi/3}^P, \bar{c}_{\pi/2} C_{\hat{T}, \pi/2}^P \right\} \quad (25)$$

Here,

$$\bar{c}_{\pi/4} = \mu_{\pi/4}^{1/2}, \quad \bar{c}_{\pi/3} = \mu_{\pi/3}^{1/2}, \quad \text{and} \quad \bar{c}_{\pi/2} = \mu_{\pi/2}^{1/2},$$

where  $\mu_{\pi/2}$  and  $\mu_{\pi/4}$  are defined in (13) and (14) and

$$\mu_{\pi/3}(\rho, \alpha) = \frac{2}{3}(1 + \rho^2 - \rho \cos \alpha) + 2\left(\frac{1}{9}(1 + \rho^2 - \rho \cos \alpha)^2 - \frac{1}{3}\rho^2 \sin^2 \alpha\right)^{1/2}, \quad (26)$$

$$\text{and } C_{\hat{T}, \pi/4}^P = \frac{1}{\sqrt{2\pi}}, \quad C_{\hat{T}, \pi/3}^P = \frac{3}{4\pi}, \quad C_{\hat{T}, \pi/2}^P = \frac{1}{\pi}.$$

**Proof:** The mapping  $\mathcal{F}_{\pi/2} : \hat{T}_{\pi/2} \rightarrow T$  coincides with (2) from Lemma 1. Therefore the bound

$$\|w\|_T \leq \bar{c}_{\pi/2} C_{\hat{T}, \pi/2}^P h \|\nabla w\|_T, \quad \bar{c}_{\pi/2}(\rho, \alpha) = \mu_{\pi/2}^{1/2}(\rho, \alpha) \quad (27)$$

is obtained by following the steps of the previous proof. From analysis of mappings

$$x = \mathcal{F}_{\pi/3}(\hat{x}) = B_{\pi/3} \hat{x}, \quad \text{where } B_{\pi/3} = \begin{pmatrix} h & \frac{h}{\sqrt{3}}(2\rho \cos \alpha - 1) - h \\ 0 & \frac{2h}{\sqrt{3}}\rho \sin \alpha \end{pmatrix}, \quad \det B_{\pi/3} = \frac{2h^2}{\sqrt{3}} \sin \alpha > 0,$$

and

$$x = \mathcal{F}_{\pi/4}(\hat{x}) = B_{\pi/4} \hat{x}, \quad \text{where } B_{\pi/4} = \begin{pmatrix} h & 2\rho h \cos \alpha - h \\ 0 & 2\rho h \sin \alpha \end{pmatrix}, \quad \det B_{\pi/4} = 2\rho h^2 \sin \alpha > 0,$$

we obtain alternative estimates for function  $w \in \tilde{H}^1(T)$

$$\|w\|_T \leq \bar{c}_{\pi/3} C_{\hat{T}, \pi/3}^P h \|\nabla w\|_T, \quad \bar{c}_{\pi/3}(\rho, \alpha) = \mu_{\pi/3}^{1/2}(\rho, \alpha), \quad (28)$$

$$\|w\|_T \leq \bar{c}_{\pi/4} C_{\hat{T}, \pi/4}^P h \|\nabla w\|_T, \quad \bar{c}_{\pi/4}(\rho, \alpha) = \mu_{\pi/4}^{1/2}(\rho, \alpha), \quad (29)$$

where  $\mu_{\pi/3}(\rho, \alpha)$  and  $\mu_{\pi/4}(\rho, \alpha)$  are defined in (26) and (14), respectively. Therefore, (25) follows from (27), (28), and (29). Analogously to Remark 2, if  $\hat{w} \in \tilde{H}^1(\hat{T})$ , it follows that  $w \in \tilde{H}^1(T)$ .  $\square$

### 3 Minorants of $C_\Gamma^P$ and $C_\Gamma^{\text{Tr}}$ for triangular domains

#### 3.1 Two-sided bounds of $C_\Gamma^P$ and $C_\Gamma^{\text{Tr}}$

Majorants of  $C_\Gamma^P$  and  $C_\Gamma^{\text{Tr}}$  provided by Lemma 1 should be compared with the corresponding minorants, which can be found by solving generalized eigenvalue problem generated by the discretized Rayleigh quotients

$$\mathcal{R}_\Gamma^P[w] = \frac{\|\nabla w\|_T}{\|w - \{w\}_\Gamma\|_T} \quad \text{and} \quad \mathcal{R}_\Gamma^{\text{Tr}}[w] = \frac{\|\nabla w\|_T}{\|w - \{w\}_\Gamma\|_\Gamma}. \quad (30)$$

Here,  $w$  is approximated by the basis of finite dimensional subspaces  $V^N \subset H^1(T)$  formed by sufficiently representative collections of test functions. For this purpose, we use either power or Fourier series and introduce

$$V_1^N := \text{span}\left\{x^i y^j\right\}, \quad \text{and} \quad V_2^N := \text{span}\left\{\cos(\pi i x) \cos(\pi j y)\right\}, \quad i, j = 0, \dots, N, \quad (i, j) \neq (0, 0),$$

with  $\dim V_1^N = \dim V_2^N = M(N) := (N + 1)^2 - 1$ . The corresponding constants are denoted by  $\underline{C}_\Gamma^{M,P}$  and  $\underline{C}_\Gamma^{M,\text{Tr}}$ , where  $M(N)$  indicates the amount of used basis functions in the finite dimensional subspace. Since above defined finite dimensional spaces are limit dense in  $H^1(T)$ , the minorants tend to exact constants as  $M(N)$  tends to infinity. The quotients (30) follow from the definition of the constants  $C_\Gamma^P$  and  $C_\Gamma^{\text{Tr}}$  for  $w \in H^1(T)$ , i.e.,

$$\|w - \{w\}_\Gamma\|_T \leq C_\Gamma^P \|\nabla w\|_T \quad \text{and} \quad \|w - \{w\}_\Gamma\|_\Gamma \leq C_\Gamma^{\text{Tr}} \|\nabla w\|_T. \quad (31)$$

Embeddings (31) are justified by the equivalence of quantity  $\|w\|_l := \|\nabla w\|_T + \left| \int_\Gamma w \, ds \right|$  to the norm of  $H^1(T)$ , so that the existence of  $C_\Gamma^P$  and  $C_\Gamma^{\text{Tr}}$  follows automatically.

Numerical results presented below are obtained with two different codes based on MATLAB Symbolic Math Toolbox [33] and The FEniCS Project [21]. Table 1 demonstrates that the ratios between exact constants and their approximate values (for the selected  $\rho$  and  $\alpha$ ) are quite close to 1 (as it is expected) even for relatively small  $N$ . Therefore, we select  $N = 6$  or  $7$  in tests discussed below.

		$\alpha = \frac{\pi}{2}, \rho = 1$		$\alpha = \frac{\pi}{4}, \rho = \frac{\sqrt{2}}{2}$	
$N$	$M(N)$	$\underline{c}_{p,\pi/2}^M$	$\underline{c}_{\text{Tr},\pi/2}^M$	$\underline{c}_{p,\pi/4}^M$	$\underline{c}_{\text{Tr},\pi/4}^M$
1	3	0.8801	0.9561	0.8647	1.0000
2	8	0.9945	0.9898	0.9925	1.0000
3	15	0.9999	0.9998	0.9962	1.0000
4	24	1.0000	0.9999	1.0000	1.0000
5	35	1.0000	1.0000	1.0000	1.0000
6	48	1.0000	1.0000	1.0000	1.0000

Table 1: Ratios of  $\underline{c}_{p,\pi/2}^M$ ,  $\underline{c}_{\text{Tr},\pi/2}^M$  and  $\underline{c}_{p,\pi/4}^M$ ,  $\underline{c}_{\text{Tr},\pi/4}^M$  with respect to increasing  $N$  and  $M(N)$ .

In Figs. 3a and 3c, we depict  $\underline{C}_\Gamma^{M,P}$  for  $M(N) = 48$  (thin line) for different  $T$  with  $\rho = \frac{\sqrt{2}}{2}$ ,  $\rho = 1$ , and  $\alpha \in (0, \pi)$ . Guaranteed upper bounds  $\overline{C}_{\pi/2}^P = c_{\pi/2}^P C_{\Gamma,\pi/2}^P$  and  $\overline{C}_{\pi/4}^P = c_{\pi/4}^P C_{\Gamma,\pi/4}^P$  are depicted by dashed lines. By the bold line, we emphasize on  $\overline{C}_{\pi/2}^P$  and  $\overline{C}_{\pi/4}^P$ , which present  $\overline{C}_\Gamma^P$  as it is defined in Lemma 1. Analogously in Figs. 4a and 4b, the lower bound  $\underline{C}_\Gamma^{M,\text{Tr}}$  (for  $M(N) = 48$ ) of the constant  $C_\Gamma^{\text{Tr}}$  is presented together with the upper bound  $\overline{C}_\Gamma^{\text{Tr}}$  (which is defined as minimum of  $\overline{C}_{\pi/2}^{\text{Tr}} = c_{\pi/2}^{\text{Tr}} C_{\widehat{\Gamma},\pi/2}^{\text{Tr}}$  and  $\overline{C}_{\pi/4}^{\text{Tr}} = c_{\pi/4}^{\text{Tr}} C_{\widehat{\Gamma},\pi/4}^{\text{Tr}}$ ; dashed lines. Parameter  $M$  is fixed to 48 since the difference of order  $1e-8$  between  $\underline{C}_\Gamma^{M,\text{Tr}}$  (for bigger  $M$ ) becomes unnoticeable. In the digital form, the information is represented in Table 2.

Fig. 3a corresponds to the case  $\rho = \frac{\sqrt{2}}{2}$ . It is worth noting that for  $\alpha = \frac{\pi}{4}$  the lower bound  $\underline{C}_\Gamma^{M,P}$  coincides with constant  $C_\Gamma^P$  ( $\overline{C}_{\pi/4}^P$ ). This happens because for  $\alpha = \frac{\pi}{4}$  the mapping  $\mathcal{F}_{\pi/4}$  is identical (see, e.g., Fig. 3b). Analogous coincidence can be observed for  $C_\Gamma^{\text{Tr}}$  ( $\overline{C}_{\pi/4}^{\text{Tr}}$ ) in Fig. 4a. In Fig. 3c, the curve corresponding to  $\underline{C}_\Gamma^{M,P}$  coincides with the line of  $C_\Gamma^P$  ( $\overline{C}_{\pi/2}^P$ ) at the point  $\alpha = \frac{\pi}{2}$  (due to the fact for this angle  $\mathcal{F}$  is the identical mapping and  $T$  coincides with  $\widehat{T}_{\pi/2}$  (see Fig. 3d)). Fig. 4b exposes similar results for  $\underline{C}_\Gamma^{M,\text{Tr}}$  and  $C_\Gamma^{\text{Tr}}$  ( $\overline{C}_{\pi/2}^{\text{Tr}}$ ). Figs. 5 and 6 demonstrate the same bounds for more interesting  $\rho = \frac{\sqrt{3}}{2}$  and  $\frac{3}{2}$ , which stay quite efficient even for the cases unrelated to the reference triangles, e.i., if  $\rho = \frac{\sqrt{3}}{2}$ ,  $I_{\text{eff}} \approx 1.0463 \div 0.1300$  for  $C_\Gamma^P$  and  $I_{\text{eff}} \approx 1.0363 \div 1.3388$  for  $C_\Gamma^{\text{Tr}}$ , and if  $\rho = \frac{3}{2}$ ,  $I_{\text{eff}} \approx 1.0249 \div 0.1634$  for  $C_\Gamma^P$  and  $I_{\text{eff}} \approx 1.2917 \div 1.7643$  for  $C_\Gamma^{\text{Tr}}$ .

$\alpha$	$\rho = \frac{\sqrt{2}}{2}$				$\rho = 1$			
	$\underline{C}_\Gamma^{48,P}$	$\overline{C}_\Gamma^P$	$\underline{C}_\Gamma^{48,Tr}$	$\overline{C}_\Gamma^{Tr}$	$\underline{C}_\Gamma^{48,P}$	$\overline{C}_\Gamma^P$	$\underline{C}_\Gamma^{48,Tr}$	$\overline{C}_\Gamma^{Tr}$
$\pi/18$	0.2429	0.2657	1.2786	1.5386	0.3245	0.3486	1.2572	1.6971
$\pi/9$	0.2414	0.2627	0.9289	1.0838	0.3248	0.3493	0.9058	1.2116
$\pi/6$	0.2389	0.2577	0.7919	0.8792	0.3268	0.3527	0.7632	1.0118
$2\pi/9$	0.2379	0.2507	0.7259	0.7543	0.3339	0.3636	0.6906	0.9201
$5\pi/18$	0.2632	0.2722	0.6945	0.7503	0.3514	0.3884	0.6529	0.9003
$\pi/3$	0.3008	0.3220	0.6829	0.8348	0.3809	0.4269	0.6362	0.8634
$7\pi/18$	0.3382	0.3694	0.6840	0.8432	0.4173	0.4721	0.6332	0.7840
$4\pi/9$	0.3740	0.4140	0.6947	0.7973	0.4556	0.5187	0.6404	0.7162
$\pi/2$	0.4075	0.4554	0.7136	0.7801	0.4929	0.4929	0.6560	0.6560
$5\pi/9$	0.4382	0.4933	0.7409	0.7973	0.5280	0.5340	0.6797	0.7162
$11\pi/18$	0.4660	0.5165	0.7779	0.8432	0.5600	0.5710	0.7125	0.7840
$2\pi/3$	0.4905	0.5361	0.8274	0.9118	0.5884	0.6037	0.7569	0.8634
$13\pi/18$	0.5115	0.5552	0.8948	1.0040	0.6129	0.6318	0.8175	0.9607
$7\pi/9$	0.5289	0.5720	0.9898	1.1292	0.6332	0.6550	0.9033	1.0874
$5\pi/6$	0.5426	0.5856	1.1334	1.3107	0.6492	0.6733	1.0332	1.2673
$8\pi/9$	0.5524	0.5956	1.3796	1.6118	0.6607	0.6865	1.2565	1.5623
$17\pi/18$	0.5583	0.6017	1.9436	2.2851	0.6676	0.6944	1.7692	2.2179

Table 2: Lower and upper bounds of  $C_\Gamma^P$  and  $C_\Gamma^{Tr}$  with respect to  $\alpha$  and for  $\rho = \frac{\sqrt{2}}{2}$  and 1.

### 3.2 Two-sided bounds of $C_T^P$

The spaces  $V_1^N$  and  $V_2^N$  are also used for analysis of the quotient  $\mathcal{R}_T[w] = \frac{\|\nabla w\|_T}{\|w - \{w\}_T\|_T}$ , which yields guaranteed lower bounds of the constant in (1) denoted by  $\underline{C}_T^{M,P}$ . Obtained numerical results are compared with above presented estimate  $\overline{C}_T^P$ ,  $\overline{C}_T^{P,\oplus} := \frac{\text{diam}(T)}{j_{1,1}}$ , and  $\underline{C}_T^P := \max\left\{\frac{\text{diam}(T)}{2j_{0,1}}, \frac{P}{4\pi}\right\}$ , which follow from (7) and (8), respectively.

In Figs. 7a, 7b, 7d, and 7e, we illustrate  $\underline{C}_T^{M,P}(M(N) = 48)$  together with  $\overline{C}_T^P$ ,  $\overline{C}_T^{P,\oplus}$  and  $\underline{C}_T^P$  with respect to  $\alpha \in (0, \pi)$  for  $T$  with  $\rho = \frac{\sqrt{2}}{2}$ ,  $\frac{\sqrt{3}}{2}$ ,  $\frac{3}{2}$ , and 2. We see that  $\underline{C}_T^{48,P}$  indeed lies within the admissible two-sided bound. From these figures, it is obvious that obtained upper bounds  $\overline{C}_T^P$  are sharper than existing estimates  $\overline{C}_T^{P,\oplus}$  for  $T$  with  $\rho \neq 1$ . True values of the constant lie between the bold and dashed lines, but closer to the bold line, which practically illustrates the constant (this follows from the fact that increasing  $M(N)$  does not provide a noticeable change for the line, e.g., for  $M(N) = 63$  maximal difference with respect to Fig. does not exceed  $1e-8$ ). Also, we note that, the lower bound  $\underline{C}_T^P$  is quite efficient, and, moreover, asymptotically exact for  $\alpha \rightarrow \pi$ .

Due to [19], we know the improved upper bound  $\overline{C}_T^{P,\Delta}$  (cf. (6)) for isosceles triangles. In Fig. 7c, we compare  $\underline{C}_T^{M,P}(M(N) = 48)$  with both upper bounds  $\overline{C}_T^P$  (from the Lemma 2) and  $\overline{C}_T^{P,\Delta}$ . It is easy to see that  $\overline{C}_T^{P,\Delta}$  is rather accurate and for  $\alpha \rightarrow 0$  and  $\alpha \rightarrow \pi$  provide almost exact estimates.  $\overline{C}_T^P$  improves  $\overline{C}_T^{P,\Delta}$  only for some  $\alpha$ . Moreover, the lower bound  $\underline{C}_T^{48}$  indeed converges to  $\overline{C}_T^{P,\Delta}$  as  $T$  degenerates when  $\alpha$  tends to 0 (see [19]).

### 3.3 Shape of the minimizer

Exact constants in (2) and (4) are generated by minimal positive eigenvalues of (3) and (5). This section presents results related to the respective eigenfunctions. In order to depict all of them in a unified form, we use barycentric coordinates  $\lambda_i \in (0, 1)$ ,  $i = 1, 2, 3$ ,  $\sum_{i=1}^3 \lambda_i = 1$ . Figs. 8 and 9 show eigenfunctions computed for isosceles triangles with different angles  $\alpha$  between two legs (zero mean condition is imposed on one of the legs). They are constructed in the process of finding  $\underline{C}_\Gamma^{M,P}$  and  $\underline{C}_\Gamma^{M,Tr}$  and normalized such that the maximal value of a function is equal to 1. For  $\alpha = \frac{\pi}{2}$ , the exact eigenfunction associated with the smallest positive eigenvalue  $\lambda_\Gamma^P = \left(\frac{z_0}{h}\right)^2$ , is known (see [25]). It is (see Fig 8d)

$$u_\Gamma^P = \cos\left(\frac{z_0 x_1}{h}\right) + \cos\left(\frac{z_0(x_2 - h)}{h}\right),$$

where  $z_0$  is the root of the first equation in (10). We can compare it with the approximate eigenfunction  $u_\Gamma^{M,P}$  computed by minimization of  $\mathcal{R}_\Gamma^P[w]$ . It is depicted in Fig. 8c.

Analogous results for eigenfunctions related to the constant  $\underline{C}_\Gamma^{M,Tr}$  are presented in Fig. 9. Again, for  $\alpha = \frac{\pi}{2}$  we know the exact one

$$u_\Gamma^{Tr} = \cos(\hat{z}_0 x_1) \cosh(\hat{z}_0(x_2 - h)) + \cosh(\hat{z}_0 x_1) \cos(\hat{z}_0(x_2 - h)),$$

where  $\hat{z}_0$  is the root of second equation in (10) (see Fig. 9d), which minimizes the quotient  $\mathcal{R}_\Gamma^{Tr}[w]$  associated with the smallest positive eigenvalue  $\lambda_\Gamma^{Tr} = \frac{\hat{z}_0 \tanh(\hat{z}_0)}{h}$ . It is easy to see that with the assigned value of  $M(N)$  numerical

approximation practically coincides with the exact one.

In the above considered examples, the eigenfunctions associated with minimal positive eigenvalues expose a continuous evolution with respect to  $\alpha$ . However, this is not true for the quotient  $\mathcal{R}_T[w]$ , where the minimizer may cardinally change the profile. Fig. 7c indicates a possibility of such rapid change at  $\alpha = \frac{\pi}{3}$ , where the curve (related to  $\underline{C}_T^{48}$ ) obviously becomes non-smooth. This happens because equilateral triangle has double eigenvalue and the function, minimizing  $\mathcal{R}_T[w]$  over  $V_1^N$ , changes its profile. Figs. 10d–10i show three eigenfunctions  $u_{T,1}^{48}$ ,  $u_{T,2}^{48}$ , and  $u_{T,3}^{48}$  related to three minimal eigenvalues  $\lambda_{T,1}^{48}$ ,  $\lambda_{T,2}^{48}$ , and  $\lambda_{T,3}^{48}$  computed in the process of minimization of  $\mathcal{R}_T[w]$ . All functions are computed for isosceles triangles and are sorted in accordance with increasing values of the respective eigenvalues. Fig. 10 illustrates these three eigenfunctions for  $T$  with angles  $\alpha = \frac{\pi}{3}$ ,  $\frac{\pi}{3} + \varepsilon$ , and  $\frac{\pi}{3} - \varepsilon$ , where  $\varepsilon = \frac{\pi}{36}$ . It is easy to see that at  $\alpha = \pi/3$  the first and the second eigenfunctions change places. Table 3 presents the corresponding results in the digital form.

It is worth noting that for equilateral triangles two minimal eigenfunctions are known (see [23]):

$$\begin{aligned} u_1 &= \cos\left(\frac{2\pi}{3}(2x_1 - 1)\right) - \cos\left(\frac{2\pi}{\sqrt{3}}x_2\right) \cos\left(\frac{\pi}{3}(2x_1 - 1)\right), \\ u_2 &= \sin\left(\frac{2\pi}{3}(2x_1 - 1)\right) + \cos\left(\frac{2\pi}{\sqrt{3}}x_2\right) \sin\left(\frac{\pi}{3}(2x_1 - 1)\right). \end{aligned}$$

These functions practically coincide with the functions  $u_{T,1}^{48}$  and  $u_{T,2}^{48}$  presented in Fig. 10d. Finally, we note that this phenomenon (change of the minimal eigenfunction) does not appear for, e.g.,  $\rho = \frac{\sqrt{2}}{2}$  or  $\rho = \frac{3}{2}$ , due to the fact that non-quadrilateral triangles have simple lowest eigenvalue. The eigenvalues as well as the constants corresponding to the eigenfunctions presented in Figs 10 are summarized in the Table 3.

		$\frac{\pi}{3} - \varepsilon$		$\frac{\pi}{3}$		$\frac{\pi}{3} + \varepsilon$	
	$u_{T,i}^M$	$\underline{C}_{T,i}^{48}$	$\lambda_{T,i}^{48}$	$\underline{C}_{T,i}^{48}$	$\lambda_{T,i}^{48}$	$\underline{C}_{T,i}^{48}$	$\lambda_{T,i}^{48}$
$\rho = 1$	$u_{T,1}^{48}$	0.2419	17.0951	0.2387	17.5463	0.2537	15.5404
	$u_{T,2}^{48}$	0.2229	20.1216	0.2387	17.5463	0.2355	18.0309
	$u_{T,3}^{48}$	0.1353	54.6024	0.1378	52.6396	0.1422	49.4818
$\rho = \frac{\sqrt{2}}{2}$	$u_{T,1}^{48}$	0.23137	18.6804	0.23671	17.8471	0.24336	16.8850
	$u_{T,2}^{48}$	0.17082	34.2707	0.17435	32.8970	0.17642	32.1295
	$u_{T,3}^{48}$	0.1229	66.2058	0.12789	61.1402	0.13298	56.5493
$\rho = \frac{3}{2}$	$u_{T,1}^{48}$	0.34714	8.2983	0.35523	7.9247	0.3648	7.5143
	$u_{T,2}^{48}$	0.24485	16.6801	0.24885	16.1482	0.25125	15.8412
	$u_{T,3}^{48}$	0.18258	29.9981	0.19084	27.4575	0.19845	25.3921

Table 3:  $\underline{C}_T^{M,P}$  and  $\lambda_T^M$  corresponding to the first three eigenfunctions in Fig. 10.

## 4 Two-sided bounds of $C_\Gamma^P$ and $C_\Gamma^{\text{Tr}}$ for tetrahedrons

A nondegenerate tetrahedron  $T \in \mathbb{R}^3$  can be presented in the form

$$T = \text{conv}\{(0, 0, 0), (h_1, 0, 0), (0, 0, h_3), (D_{x_1}, D_{x_2}, D_{x_3})\}, \quad (32)$$

where  $(D_{x_1}, D_{x_2}, D_{x_3}) = (h_1\rho \cos \alpha \sin \theta, h_1\rho \sin \alpha \sin \theta, h_1\rho \cos(\theta))$ ,  $h_1$  and  $h_3$  are the scaling parameters along axes  $O_{x_1}$  and  $O_{x_3}$ , respectively,  $\alpha$  is a polar angle, and  $\theta$  is an azimuthal angle (see Fig. 2). Let zero mean condition be imposed on

$$\Gamma = \text{conv}\{(0, 0, 0), (h_1, 0, 0), (0, 0, h_3)\},$$

and  $\hat{T}_{\hat{\theta}, \hat{\alpha}}$  denote the reference tetrahedron, where  $\hat{\theta}$  and  $\hat{\alpha}$  are fixed angles. Then, by  $\mathcal{F}_{\hat{\theta}, \hat{\alpha}}$  we denote the respective mapping  $\mathcal{F}_{\hat{\theta}, \hat{\alpha}}: \hat{T}_{\hat{\theta}, \hat{\alpha}} \rightarrow T$ .

It is possible that these results could be generalized to the other spectral problems that authors consider. To the best of our knowledge, exact values of constants in Poincaré-type inequalities for simplexes in  $\mathbb{R}^3$  are unknown. Therefore, we first consider several reference tetrahedrons with  $\rho = 1$ ,  $\hat{\theta} = \frac{\pi}{2}$ , and  $\hat{\alpha}_1 = \frac{\pi}{4}$ ,  $\hat{\alpha}_2 = \frac{\pi}{3}$ ,  $\hat{\alpha}_3 = \frac{\pi}{2}$ , and  $\hat{\alpha}_4 = \frac{2\pi}{3}$ , and find the constants numerically with high accuracy. Table 4 shows convergence of the constants with respect to increasing  $M(N)$ . Then, for an arbitrary tetrahedron  $T$ , we have

$$\begin{aligned} \|v\|_T &\leq \tilde{C}_\Gamma^P h_1 h_3 \|\nabla v\|_T, \quad \tilde{C}_\Gamma^P = \min_{\hat{\alpha} = \{\pi/4, \pi/3, \pi/2, 2\pi/3\}} \left\{ c_{\pi/2, \hat{\alpha}}^P C_{\hat{\Gamma}, \pi/2, \hat{\alpha}}^P \right\}, \\ \|v\|_\Gamma &\leq \tilde{C}_\Gamma^{\text{Tr}} (h_1 h_3)^{\frac{1}{2}} \|\nabla v\|_T, \quad \tilde{C}_\Gamma^{\text{Tr}} = \min_{\hat{\alpha} = \{\pi/4, \pi/3, \pi/2, 2\pi/3\}} \left\{ c_{\pi/2, \hat{\alpha}}^{\text{Tr}} C_{\hat{\Gamma}, \pi/2, \hat{\alpha}}^{\text{Tr}} \right\}, \end{aligned} \quad (33)$$

	$\hat{\theta} = \frac{\pi}{2}, \hat{\alpha} = \frac{\pi}{4}$	$\hat{\theta} = \frac{\pi}{2}, \hat{\alpha} = \frac{\pi}{3}$	$\hat{\theta} = \frac{\pi}{2}, \hat{\alpha} = \frac{\pi}{2}$	$\hat{\theta} = \frac{\pi}{2}, \hat{\alpha} = \frac{2\pi}{3}$				
$M(N)$	$C_{\hat{\Gamma}, \pi/2, \hat{\alpha}}^{\text{P}, M}$	$C_{\hat{\Gamma}, \pi/2, \hat{\alpha}}^{\text{Tr}, M}$	$C_{\hat{\Gamma}, \pi/2, \hat{\alpha}}^{\text{P}, M}$	$C_{\hat{\Gamma}, \pi/2, \hat{\alpha}}^{\text{Tr}, M}$	$C_{\hat{\Gamma}, \pi/2, \hat{\alpha}}^{\text{P}, M}$	$C_{\hat{\Gamma}, \pi/2, \hat{\alpha}}^{\text{Tr}, M}$	$C_{\hat{\Gamma}, \pi/2, \hat{\alpha}}^{\text{P}, M}$	$C_{\hat{\Gamma}, \pi/2, \hat{\alpha}}^{\text{Tr}, M}$
7	0.32431	0.760099	0.325985	0.654654	0.360532	0.654654	0.4152099	0.686161
26	0.338539	0.829445	0.340267	0.761278	0.373669	0.751615	0.4274757	0.863324
63	0.341122	0.831325	0.342556	0.762901	0.375590	0.751994	0.4286444	0.864595
124	0.341147	0.831335	0.342589	0.762905	0.375603	0.751999	0.4286652	0.864630
215	<b>0.341147</b>	<b>0.831335</b>	<b>0.342589</b>	<b>0.762905</b>	<b>0.375603</b>	<b>0.751999</b>	<b>0.4286652</b>	<b>0.864630</b>

Table 4:  $C_{\hat{\Gamma}, \pi/2, \hat{\alpha}}^{\text{P}, M}$  and  $C_{\hat{\Gamma}, \pi/2, \hat{\alpha}}^{\text{Tr}, M}$  with respect to  $M(N)$  for  $\hat{T}_{\hat{\theta}, \hat{\alpha}}$  with  $\rho = 1$ ,  $\hat{\theta} = \frac{\pi}{2}$ , and several  $\hat{\alpha}$ .

where  $C_{\hat{\Gamma}, \pi/2, \hat{\alpha}}^{\text{P}}$  and  $C_{\hat{\Gamma}, \pi/2, \hat{\alpha}}^{\text{Tr}}$  are the constants related to four reference tetrahedron from Table 4 and  $c_{\pi/2, \hat{\alpha}}^{\text{P}}$  and  $c_{\pi/2, \hat{\alpha}}^{\text{Tr}}$  are the ratios of the mapping  $\mathcal{F}_{\pi/2, \hat{\alpha}}: \hat{T}_{\pi/2, \hat{\alpha}} \rightarrow T$ . Here,  $\hat{T}_{\pi/2, \hat{\alpha}} := \text{conv}\{(0, 0, 0), (1, 0, 0), (0, 0, 1), (\cos \hat{\alpha}, \sin \hat{\alpha}, 0)\}$  with  $\hat{\alpha} = \{\frac{\pi}{4}, \frac{\pi}{3}, \frac{\pi}{2}, \frac{2\pi}{3}\}$ ,  $T$  is defined in (32), and  $\mathcal{F}_{\pi/2, \hat{\alpha}}(\hat{x})$  is presented by the relation

$$x = \mathcal{F}_{\pi/2, \hat{\alpha}}(\hat{x}) = B_{\pi/2, \hat{\alpha}} \hat{x}, \quad B_{\pi/2, \hat{\alpha}} = \begin{pmatrix} h_1 & \frac{h_1}{\sin \hat{\alpha}} (\rho \cos \alpha \sin \theta - \cos \hat{\alpha}) & 0 \\ 0 & h_1 \rho \frac{\sin \alpha \sin(\theta)}{\sin \hat{\alpha}} & 0 \\ 0 & h_1 \rho \frac{\cos \theta}{\sin \hat{\alpha}} & h_3 \end{pmatrix}. \quad (34)$$

The mapping ratios of (34) depend on the maximum eigenvalue of the matrix

$$A_{\pi/2, \hat{\alpha}} := \begin{pmatrix} h_1^2 + b_{12}^2 & b_{12}b_{22} & b_{12}b_{32} \\ b_{12}b_{22} & b_{22}^2 & b_{22}b_{32} \\ b_{12}b_{32} & b_{22}b_{32} & h_3^2 + b_{32}^2 \end{pmatrix}$$

$$= h_1^2 \cdot \begin{pmatrix} 1 + \frac{1}{\sin^2 \hat{\alpha}} (\rho \cos \alpha \sin \theta - \cos \hat{\alpha})^2 & \frac{\rho \sin \alpha \sin \theta}{\sin^2 \hat{\alpha}} (\rho \cos \alpha \sin \theta - \cos \hat{\alpha}) & \frac{\rho \cos \theta}{\sin^2 \hat{\alpha}} (\rho \cos \alpha \sin \theta - \cos \hat{\alpha}) \\ \frac{\rho \sin \alpha \sin \theta}{\sin^2 \hat{\alpha}} (\rho \cos \alpha \sin \theta - \cos \hat{\alpha}) & \frac{\rho^2 \sin^2 \alpha \cos^2 \theta}{\sin^2 \hat{\alpha}} & \frac{\rho^2 \sin \alpha \sin 2\theta}{2 \sin^2 \hat{\alpha}} \\ \frac{\rho \cos \theta}{\sin^2 \hat{\alpha}} (\rho \cos \alpha \sin \theta - \cos \hat{\alpha}) & \frac{\rho^2 \sin \alpha \sin 2\theta}{2 \sin^2 \hat{\alpha}} & \frac{h_3^2}{h_1^2} + \rho^2 \frac{\cos^2 \theta}{\sin^2 \hat{\alpha}} \end{pmatrix},$$

where  $b_{12}$ ,  $b_{22}$ ,  $b_{32}$  are elements of  $B_{\pi/2, \hat{\alpha}}$  in (34). Accordingly,  $\lambda_{\max}(A_{\pi/2, \hat{\alpha}})$  is defined by the relation

$$\lambda_{\max}(A_{\pi/2, \hat{\alpha}}) = \mu_{\pi/2, \hat{\alpha}} = \mathcal{E}_4^{1/3} - \mathcal{E}_2 \mathcal{E}_4^{-1/3} + \frac{1}{2} \mathcal{E}_1,$$

where

$$\begin{aligned} \mathcal{E}_1 &= b_{12}^2 + b_{22}^2 + b_{32}^2 + h_1^2 + h_3^2, \\ \mathcal{E}_2 &= \frac{1}{3} \left( h_3^2 (b_{12}^2 + b_{22}^2) + h_1^2 (b_{22}^2 + b_{32}^2) - \frac{1}{3} \mathcal{E}_1^2 + h_1^2 h_3^2 \right), \\ \mathcal{E}_3 &= \frac{1}{27} \mathcal{E}_1^3 - \frac{1}{6} \mathcal{E}_1 \left( h_3^2 (b_{12}^2 + b_{22}^2) + h_1^2 (b_{22}^2 + b_{32}^2) + h_1^2 h_3^2 \right) + \frac{1}{2} b_{22}^2 h_1^2 h_3^2, \\ \mathcal{E}_4 &= \mathcal{E}_3 + \left( \left( \frac{h_3^2}{3} (b_{12}^2 + b_{22}^2) + \frac{h_1^2}{3} (b_{22}^2 + b_{32}^2) - \frac{1}{9} \mathcal{E}_1^2 + \frac{1}{3} h_1^2 h_3^2 \right)^3 + \mathcal{E}_3^2 \right)^{1/2}. \end{aligned}$$

Therefore,  $c_{\pi/2, \hat{\alpha}}^{\text{P}}$  and  $c_{\pi/2, \hat{\alpha}}^{\text{Tr}}$  in (33) reads as follows

$$c_{\pi/2, \hat{\alpha}}^{\text{P}} = \frac{\mu_{\pi/2, \hat{\alpha}}^{1/2}}{h_1 h_3}, \quad c_{\pi/2, \hat{\alpha}}^{\text{Tr}} = \left( \frac{h_3 \sin \hat{\alpha}}{\rho \sin \alpha \sin \theta} \right)^{1/2} c_{\pi/2, \hat{\alpha}}^{\text{P}}.$$

Lower bounds of the constants  $C_{\Gamma}^{\text{P}}$  and  $C_{\Gamma}^{\text{Tr}}$  are computed by minimization of  $\mathcal{R}_{\Gamma}^{\text{P}}[w]$  and  $\mathcal{R}_{\Gamma}^{\text{Tr}}[w]$  over the set  $V_3^N \subset H^1(T)$ , where

$$V_3^N := \left\{ \varphi_{ijk} = x^i y^j z^k, \quad i, j, k = 0, \dots, N, \quad (i, j, k) \neq (0, 0, 0) \right\}, \quad \dim V_3^N = M(N) := (N+1)^3 - 1.$$

The respective results are presented in Tables 5 and 6 for  $T$  with  $h_1 = 1$ ,  $h_3 = 1$ , and  $\rho = 1$ . We note that exact values of constants are probably closer to the numbers presented in left-hand side columns. For a fixed angle  $\theta = \pi/2$ , we also present estimates of  $\underline{C}_\Gamma^{M,P}$  and  $\underline{C}_\Gamma^{M,Tr}$  graphically in Fig. 11.

	$\alpha = \frac{\pi}{6}$		$\alpha = \frac{\pi}{4}$		$\alpha = \frac{\pi}{3}$		$\alpha = \frac{\pi}{2}$	
$\theta$	$\underline{C}_\Gamma^{M,P}$	$\tilde{C}_\Gamma^P$	$\underline{C}_\Gamma^{M,P}$	$\tilde{C}_\Gamma^P$	$\underline{C}_\Gamma^{M,P}$	$\tilde{C}_\Gamma^P$	$\underline{C}_\Gamma^{M,P}$	$\tilde{C}_\Gamma^P$
$\pi/6$	0.23883	0.49035	0.24621	0.49841	0.25870	0.51054	0.29484	0.51308
$\pi/4$	0.23883	0.45388	0.24621	0.46173	0.25870	0.47683	0.29484	0.49075
$\pi/3$	0.29666	0.41958	0.31194	0.42259	0.33489	0.43724	0.38976	0.46002
$\pi/2$	0.34302	0.35667	0.34112	0.34115	0.34256	0.34259	0.37559	0.37560
$2\pi/3$	0.40428	0.41958	0.40562	0.42259	0.40927	0.43724	0.42867	0.46002
$3\pi/4$	0.42890	0.45388	0.43110	0.46173	0.43505	0.47683	0.45017	0.49075
$5\pi/6$	0.44964	0.49035	0.45193	0.49841	0.45539	0.51054	0.46607	0.51308
	$\alpha = \frac{\pi}{2}$		$\alpha = \frac{2\pi}{3}$		$\alpha = \frac{3\pi}{4}$		$\alpha = \frac{5\pi}{6}$	
$\theta$	$\underline{C}_\Gamma^{M,P}$	$\tilde{C}_\Gamma^P$	$\underline{C}_\Gamma^{M,P}$	$\tilde{C}_\Gamma^P$	$\underline{C}_\Gamma^{M,P}$	$\tilde{C}_\Gamma^P$	$\underline{C}_\Gamma^{M,P}$	$\tilde{C}_\Gamma^P$
$\pi/6$	0.29484	0.51308	0.33069	0.51792	0.34468	0.52253	0.35499	0.52694
$\pi/4$	0.29484	0.49075	0.33069	0.50261	0.34468	0.51308	0.35499	0.52253
$\pi/3$	0.38976	0.46002	0.43880	0.48413	0.45742	0.50261	0.47106	0.51792
$\pi/2$	0.37559	0.37560	0.42865	0.42867	0.45017	0.45731	0.46607	0.47811
$2\pi/3$	0.42867	0.46002	0.45997	0.48413	0.47457	0.50261	0.48598	0.51792
$3\pi/4$	0.45017	0.49075	0.47204	0.50261	0.48239	0.51308	0.49064	0.52253
$5\pi/6$	0.46607	0.51308	0.47972	0.51792	0.48607	0.52253	0.49115	0.52694

Table 5:  $\underline{C}_\Gamma^{M,P}(M(N) = 124)$  and  $\tilde{C}_\Gamma^P$ .

	$\alpha = \frac{\pi}{6}$		$\alpha = \frac{\pi}{4}$		$\alpha = \frac{\pi}{3}$		$\alpha = \frac{\pi}{2}$	
$\theta$	$\underline{C}_\Gamma^{M,Tr}$	$\tilde{C}_\Gamma^{Tr}$	$\underline{C}_\Gamma^{M,Tr}$	$\tilde{C}_\Gamma^{Tr}$	$\underline{C}_\Gamma^{M,Tr}$	$\tilde{C}_\Gamma^{Tr}$	$\underline{C}_\Gamma^{M,Tr}$	$\tilde{C}_\Gamma^{Tr}$
$\pi/6$	1.09760	3.78259	0.96245	2.71866	0.91255	2.27382	0.93123	2.05449
$\pi/4$	1.09760	2.43897	0.96245	1.78094	0.91255	1.50166	0.93123	1.38951
$\pi/3$	0.89122	1.74467	0.79146	1.31130	0.75950	1.12431	0.78904	1.06349
$\pi/2$	0.98017	1.22920	0.83132	0.83133	0.76290	0.76291	0.75199	0.75200
$2\pi/3$	1.17698	1.74467	0.99473	1.31130	0.90578	1.12431	0.86463	1.06349
$3\pi/4$	1.35195	2.43897	1.14144	1.78094	1.03737	1.50166	0.98220	1.38951
$5\pi/6$	1.65317	3.78259	1.39424	2.71866	1.26490	2.27382	1.19017	2.05449
	$\alpha = \frac{\pi}{2}$		$\alpha = \frac{2\pi}{3}$		$\alpha = \frac{3\pi}{4}$		$\alpha = \frac{5\pi}{6}$	
$\theta$	$\underline{C}_\Gamma^{M,Tr}$	$\tilde{C}_\Gamma^{Tr}$	$\underline{C}_\Gamma^{M,Tr}$	$\tilde{C}_\Gamma^{Tr}$	$\underline{C}_\Gamma^{M,Tr}$	$\tilde{C}_\Gamma^{Tr}$	$\underline{C}_\Gamma^{M,Tr}$	$\tilde{C}_\Gamma^{Tr}$
$\pi/6$	0.93123	2.05449	1.07244	2.39471	1.21573	2.95902	1.47044	4.21999
$\pi/4$	0.93123	1.38951	1.07244	1.64324	1.21573	2.01841	1.47044	2.80588
$\pi/3$	0.78904	1.06349	0.91773	1.27423	1.04309	1.50833	1.26357	2.11790
$\pi/2$	0.75199	0.75200	0.86459	0.86463	0.98220	1.12971	1.19017	1.67033
$2\pi/3$	0.86463	1.06349	0.96174	1.27423	1.08134	1.50833	1.30191	2.11790
$3\pi/4$	0.98220	1.38951	1.07921	1.64324	1.20686	2.01841	1.44721	2.80588
$5\pi/6$	1.19017	2.05449	1.29582	2.39471	1.44268	2.95902	1.72383	4.21999

Table 6:  $\underline{C}_\Gamma^{M,Tr}(M(N) = 124)$  and  $\tilde{C}_\Gamma^{Tr}$ .

## 5 Example

Constants in the Friedrichs', Poincaré, and other functional inequalities arise in various problems of numerical analysis, where we need to know values of the respective constants associated with particular domains. For example, results related to extension and projection type estimates for FEM can be found in [24, 7] (and many other publications). Concerning constants in the trace inequalities associated with polygonal domain, we mention the paper [5]. Constants in functional (embedding) inequalities arise in various error estimates. We deduce an advanced version of the estimate (46) in [31], which uses constants in Poincaré-type inequalities for functions with zero mean traces on inter-element boundaries in order to maximally extend the space of admissible fluxes. Below we address the latter case and first explain reasons that invoke the constants in general terms.

Let  $u$  denote the exact solution of an elliptic boundary value problem generated by the pair of conjugate operators grad and  $-\text{div}$  (e.g., the problem (38)–(41) considered below) and  $v$  be a function in the energy space satisfying the prescribed (Dirichlet) boundary conditions. Typically, the error  $e := u - v$  is measured in terms of the energy

norm  $\|\nabla e\|$  (or some other equivalent norm), which square is bounded from above by the quantities

$$\int_{\Omega} R(v, \operatorname{div} q) e \, dx, \quad \int_{\Omega} D(\nabla v, q) \cdot \nabla e \, dx, \quad \text{and} \quad \int_{\Gamma_N} R_{\Gamma_N}(v, q \cdot n) e \, ds,$$

where  $\Gamma_N$  is the Neumann part of the boundary  $\partial T$ ,  $n$  is the outward unit normal, and  $q$  is an approximation of the dual variable (flux). The terms  $R$ ,  $D$ , and  $R_{\Gamma_N}$  represent residuals of the differential (balance) equation, constitutive (duality) relation, and Neumann boundary condition, respectively. Since  $v$  and  $q$  are known from a numerical solution, fully computable estimates can be obtained if these integrals are estimated by the Hölder, Friedrichs, and trace inequalities (which involve the corresponding constants). However, for a Lipschitz domain  $\Omega$  with piecewise smooth (e.g., polynomial) boundaries these constants may be unknown. A way to avoid these difficulties is suggested by modifications of the estimates using ideas of domain decomposition. Assume that  $\Omega$  is polygonal (polyhedral) domain decomposed into a collection of non-overlapping convex polygonal sub-domains  $\Omega_i$ , i.e.,

$$\bar{\Omega} := \bigcup_{\Omega_i \in \mathcal{O}_{\Omega}} \bar{\Omega}_i, \quad \mathcal{O}_{\Omega} := \left\{ \Omega_i \in \Omega \mid \Omega_{i'} \cap \Omega_{i''} = \emptyset, \, i' \neq i'', \, i = 1, \dots, N \right\}.$$

We denote the set of all edges (faces) by  $\mathcal{G}$  and the set of all interior faces by  $\mathcal{G}_{\text{int}}$  (i.e.,  $\Gamma_{ij} \in \mathcal{G}_{\text{int}}$ , if  $\Gamma_{ij} = \bar{\Omega}_i \cap \bar{\Omega}_j$ ). Analogously,  $\mathcal{G}_N$  denotes the set of edges on  $\Gamma_N$ . The latter set is decomposed into  $\Gamma_{N_k} := \Gamma_N \cap \partial\Omega_k$  (the number of faces that belongs to  $\Gamma_{N_k}$  is  $K_N$ ). Now, the integrals associated with  $R$  and  $R_{\Gamma_N}$  can be replaced by sums of local quantities

$$\sum_{i=1}^N \int_{\Omega_i} R_{\Omega_i}(v, \operatorname{div} q) e \, dx, \quad \text{and} \quad \sum_{k=1}^{K_N} \int_{\Gamma_{N_k}} R_{\Gamma_N}(v, q \cdot n) e \, ds.$$

If the residuals satisfy the conditions

$$\int_{\Omega_i} R_{\Omega_i}(v, \operatorname{div} q) \, dx = 0, \quad \forall i = 1, \dots, N,$$

and

$$\int_{\Gamma_{N_k}} R_{\Gamma_N}(v, q \cdot n) \, ds = 0, \quad \forall k = 1, \dots, K_N,$$

then

$$\int_{\Omega_i} R_{\Omega_i}(v, \operatorname{div} q) e \, dx \leq C_{\Omega_i}^{\text{P}} \|R_{\Omega_i}(v, \operatorname{div} q)\|_{\Omega_i} \|\nabla e\|_{\Omega_i}, \quad (35)$$

and

$$\int_{\Gamma_{N_k}} R_{\Gamma_N}(v, q \cdot n) e \, ds \leq C_{\Gamma_{N_k}}^{\text{Tr}} \|R_{\Gamma_N}(v, q \cdot n)\|_{\Gamma_{N_k}} \|\nabla e\|_{\Omega_k}. \quad (36)$$

Hence, we can deduce a computable upper bound of the error that contains local constants  $C_{\Omega_i}^{\text{P}}$  and  $C_{\Gamma_{N_k}}^{\text{Tr}}$  for simple subdomains (e.g., triangles or tetrahedrons) instead of the global constants associated with  $\Omega$ .

The constant  $C_{\Omega}^{\text{P}}$  may arise if, e.g., nonconforming approximations are used. For example, if  $v$  does not exactly satisfy the Dirichlet boundary condition on  $\Gamma_{D_k}$ , then in the process of estimation it may be necessary to evaluate terms of the type

$$\int_{\Gamma_{D_k}} G_D(v) e \, ds, \quad k = 1, \dots, K_D,$$

where  $\Gamma_{D_k}$  is a part of  $\Gamma_D$  associated with a certain  $\Omega_k$ , and  $G_D(v)$  is a residual generated by inexact satisfaction of the boundary condition. If we impose the requirement that the Dirichlet boundary condition is satisfied in a weak sense, i.e.,  $\{G_D(v)\}_{\Gamma_{D_k}} = 0$ , then each boundary integral can be estimated as follows:

$$\int_{\Gamma_{D_k}} G_D(v) e \, ds \leq C_{\Gamma_{D_k}}^{\text{P}} \|G_D(v)\|_{\Gamma_{D_k}} \|\nabla e\|_{\Omega_k}. \quad (37)$$

After summing (35), (36), and (37), we obtain a product of weighted norms of localized residuals (which are known) and  $\|\nabla e\|_{\Omega}$ . Since the sum is bounded from below by the squared energy norm, we arrive at computable error majorant.

Now, we discuss elaborately these questions with the paradigm of the following boundary value problem: find  $u$  such that

$$-\operatorname{div} p + \varrho^2 u = f, \quad \text{in } \Omega, \quad (38)$$

$$p = A \nabla u, \quad \text{in } \Omega, \quad (39)$$

$$u = u_D, \quad \text{on } \Gamma_D, \quad (40)$$

$$A \nabla u \cdot n = F \quad \text{on } \Gamma_N. \quad (41)$$

Here  $f \in L^2(\Omega)$ ,  $F \in L^2(\Gamma_N)$ ,  $u_D \in H^1(\Omega)$ , and  $A$  is a symmetric positive definite matrix with bounded coefficients satisfying the condition  $\lambda_1 |\xi|^2 \leq A \xi \cdot \xi$ , where  $\lambda_1$  is a positive constant independent of  $\xi$ . The generalized solution of (38)–(41) exists and is unique in the set  $V_0 + u_D$ , where  $V_0 := \{w \in H^1(\Omega) \mid w = 0 \text{ on } \Gamma_D\}$ .

Assume that  $v \in V_0 + u_D$  is a conforming approximation of  $u$ . We wish to find a computable majorant of the error norm

$$\|e\|^2 := \|\nabla e\|_A^2 + \|\varrho e\|^2, \quad (42)$$

where  $\|\nabla e\|_A^2 := \int_{\Omega} A \nabla e \cdot \nabla e \, dx$ . First, we note that the integral identity that defines  $u$  can be rewritten in the form

$$\int_{\Omega} A \nabla e \cdot \nabla w \, dx + \int_{\Omega} \varrho^2 e w \, dx = \int_{\Omega} (f w - \varrho^2 v w - A \nabla v \cdot \nabla w) \, dx + \int_{\Gamma_N} F w \, ds, \quad \forall w \in V_0. \quad (43)$$

It is well known (see [31, Section 4.2]) that this relation yields computable majorant of  $\|e\|^2$ , if we introduce a vector valued function  $q \in H(\Omega, \operatorname{div})$  and transform (43) by means of integration by parts relations. The majorant has the form

$$\|e\| \leq \|D_{\Omega}(\nabla v, q)\|_{A^{-1}} + C_1 \|R(v, \operatorname{div} q)\|_{\Omega} + C_2 \|R_{\Gamma_N}(v, q \cdot n)\|_{\Gamma_N}, \quad (44)$$

where  $C_1$  and  $C_2$  are positive constants explicitly defined by  $\lambda_1$ , the Friedrichs' inequality  $C_{\Omega}^F$  in  $\|v\|_{\Omega} \leq C_{\Omega}^F \|\nabla v\|_{\Omega}$  for functions vanishing on  $\Gamma_D$ , and constant  $C_{\Gamma_N}^{\operatorname{Tr}}$  in the trace inequality associated with  $\Gamma_N$ . The integrands are defined by the relations

$$D(\nabla v, q) := A \nabla v - q, \quad R(v, \operatorname{div} q) := \operatorname{div} q + f - \varrho^2 v, \quad \text{and} \quad R_{\Gamma_N}(v, q \cdot n) := q \cdot n - F.$$

In general, finding  $C_{\Omega}^F$  and  $C_{\Gamma_N}^{\operatorname{Tr}}$  may be not an easy task. We can exclude  $C_2$  if  $q$  additionally satisfies the condition  $q \cdot n = F$ . Then, the last term in (44) vanishes. However, this condition is difficult to satisfy, if  $F$  is a complicated nonlinear function. In order to exclude  $C_1$ , we can apply domain decomposition and use (35) instead of the global estimate. Then, the estimate will operate with the constants  $C_{\Omega_i}^P$  (which upper bounds are known for convex domains). Moreover, it is shown below that using the inequalities (2) and (4), we can essentially weaken the assumptions required for the variable  $q$ .

Define the space of vector valued functions

$$\begin{aligned} \hat{H}(\Omega, \mathcal{O}_{\Omega}, \operatorname{div}) := \left\{ q \in L^2(\Omega, \mathbb{R}^d) \mid \right. & q = q_i \in H(\Omega_i, \operatorname{div}), \\ & \left. \left\{ \operatorname{div} q_i + f - \varrho^2 v \right\}_{\Omega_i} = 0, \quad \forall \Omega_i \in \mathcal{O}_{\Omega}, \right. \\ & \left. \left\{ (q_i - q_j) \cdot n_{ij} \right\}_{\Gamma_{ij}} = 0, \quad \forall \Gamma_{ij} \in \mathcal{G}_{\operatorname{int}}, \right. \\ & \left. \left\{ q_i \cdot n_k - F \right\}_{\Gamma_{N_k}} = 0, \quad \forall k = 1, \dots, K_N \right\}. \end{aligned}$$

We note that the space  $\hat{H}(\Omega, \mathcal{O}_{\Omega}, \operatorname{div})$  is wider than  $H(\Omega, \operatorname{div})$  (so that we have more flexibility in determination of optimal reconstruction of numerical fluxes). Indeed, the vector valued functions in  $H(\Omega, \operatorname{div})$  must have continuous normal components on all  $\Gamma_{ij} \in \mathcal{G}_{\operatorname{int}}$  and satisfy the Neumann boundary condition in the pointwise sense. The functions in  $\hat{H}(\Omega, \mathcal{O}_{\Omega}, \operatorname{div})$  satisfy much weaker conditions: namely, the normal components are continuous only in terms of mean values (integrals) and the Neumann condition must hold in the integral sense only.

We reform (43) by means of the integral identity

$$\sum_{\Omega_i \in \mathcal{O}_{\Omega}} \int_{\Omega_i} (q \cdot \nabla w + \operatorname{div} q w) \, dx = \sum_{\Gamma_{ij} \in \mathcal{G}_{\operatorname{int}}} \int_{\Gamma_{ij}} (q_i - q_j) \cdot n_{ij} w \, ds + \sum_{\Gamma_{N_k} \in \Gamma_N} \int_{\Gamma_{N_k}} q_i \cdot n_i w \, ds,$$

which holds for any  $w \in V_0$  and  $q \in \hat{H}(\Omega, \mathcal{O}_\Omega, \text{div})$ . Setting  $w = e$  in (43) and applying the Hölder inequality, we find that

$$\begin{aligned} \|e\|^2 \leq & \|D(\nabla v, q)\|_{A^{-1}} \|\nabla e\|_A + \sum_{\Omega_i \in \mathcal{O}_\Omega} \|R(v, \text{div} q)\|_{\Omega_i} \|e - \{e\}_{\Omega_i}\|_{\Omega_i} \\ & + \sum_{\Gamma_{ij} \in \mathcal{G}_{\text{int}}} r_{ij}(q) \|e - \{e\}_{\Gamma_{ij}}\|_{\Gamma_{ij}} + \sum_{\Gamma_{N_k} \in \Gamma_N} \rho_k(q) \|e - \{e\}_{\Gamma_{N_k}}\|_{\Gamma_{N_k}}, \end{aligned}$$

where

$$r_{ij}(q) := \|(q_i - q_j) \cdot n_{ij}\|_{\Gamma_{ij}}, \quad \rho_k(q) := \|q_k \cdot n_k - F\|_{\Gamma_{N_k}}.$$

In view of (1) and (4), we obtain

$$\begin{aligned} \|e\|^2 \leq & \|D(\nabla v, q)\|_{A^{-1}} \|\nabla e\|_A + \sum_{\Omega_i \in \mathcal{O}_\Omega} \|R(v, \text{div} q)\|_{\Omega_i} C_{\Omega_i}^{\text{P}} \|\nabla e\|_{\Omega_i} \\ & + \sum_{\Gamma_{ij} \in \mathcal{G}_{\text{int}}} r_{ij}(q) C_{\Gamma_{ij}}^{\text{Tr}} \|\nabla e\|_{\Omega_i} + \sum_{\Gamma_{N_k} \in \Gamma_N} \rho_k(q) C_{\Gamma_{N_k}}^{\text{Tr}} \|\nabla e\|_{\Omega_i}. \quad (45) \end{aligned}$$

The second term in the right hand side is estimated by the quantity  $\mathfrak{R}_1(v, q) \|\nabla e\|_\Omega$ , where

$$\mathfrak{R}_1^2(v, q) := \sum_{\Omega_i \in \mathcal{O}_\Omega} \frac{(\text{diam } \Omega_i)^2}{\pi^2} \|R(v, \text{div} q)\|_{\Omega_i}^2.$$

We can represent any  $\Omega_i \in \mathcal{O}_\Omega$  as a sum of simplexes such that each simplex has one edge on  $\partial\Omega_i$ . Let  $C_{i, \max}^{\text{Tr}}$  denote the largest constant in the respective Poincaré-type inequalities (4) associated with all edges of  $\partial\Omega_i$ . Then, the last two terms of (45) can be estimated by the quantity  $\mathfrak{R}_2(v, q) \|\nabla e\|_\Omega$ , where

$$\mathfrak{R}_2^2(q) := \sum_{\Omega_i \in \mathcal{O}_\Omega} (C_{i, \max}^{\text{Tr}})^2 \eta_i^2, \quad \text{with } \eta_i^2 = \sum_{\substack{\Gamma_{ij} \in \mathcal{G}_{\text{int}}, \\ \Gamma_{ij} \cap \partial\Omega_i \neq \emptyset}} \frac{1}{4} r_{ij}^2(q) + \sum_{\substack{\Gamma_k \in \mathcal{G}_N, \\ \Gamma_k \cap \partial\Omega_i \neq \emptyset}} \rho_k^2(q).$$

Then, (45) yields the estimate

$$\|e\|^2 \leq \|D(\nabla v, q)\|_{A^{-1}} \|\nabla e\|_A + (\mathfrak{R}_1(v, q) + \mathfrak{R}_2(q)) \|\nabla e\|_\Omega,$$

which shows that

$$\|e\| \leq \|D(\nabla v, q)\|_{A^{-1}} + \frac{1}{\lambda_1} (\mathfrak{R}_1(v, q) + \mathfrak{R}_2(q)). \quad (46)$$

Here, the term  $\mathfrak{R}_2(q)$  controls violations of conformity of  $q$  (on interior edges) and inexact satisfaction of boundary conditions (on edges related to  $\Gamma_N$ ). It is easy to see that  $\mathfrak{R}_2(q) = 0$ , if and only if  $q \cdot n$  is continuous on  $\mathcal{G}_{\text{int}}$  and exactly satisfy the boundary condition. Hence, it can be viewed as a measure of the “flux nonconformity”. Other terms have the same meaning as in known a posteriori estimates of the functional type, namely, the first term measures the violation in the relation  $q = A \nabla v$  (cf. (39)), and  $\mathfrak{R}_1(v, q)$  measures inaccuracy in the equilibrium (balance) equation (38). The right-hand side of (46) contains known functions (approximation  $v$  and the reconstruction of the flux  $q$ ) and constants that can be easily computed using results of Section 2-4. Finally, we note that estimates similar to (46) were derived in [32] for elliptic variational inequalities and in [22] for a class of parabolic problems.

# 6 Appendix

For convenience, we collect in this part the graphics cited in Section 3 and 4.

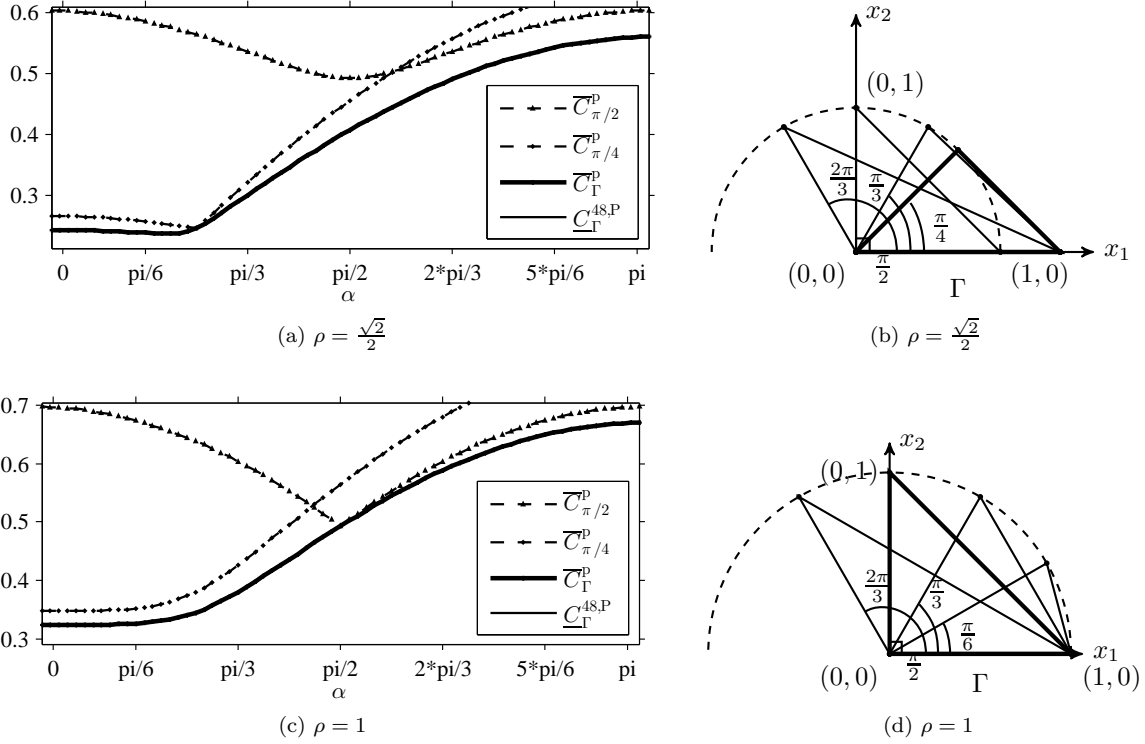


Figure 3: Lower and upper bounds of  $C_\Gamma^P$  for  $T \in \mathbb{R}^2$  (a)-(b)  $\rho = \frac{\sqrt{2}}{2}$  and (c)-(d)  $\rho = 1$ .

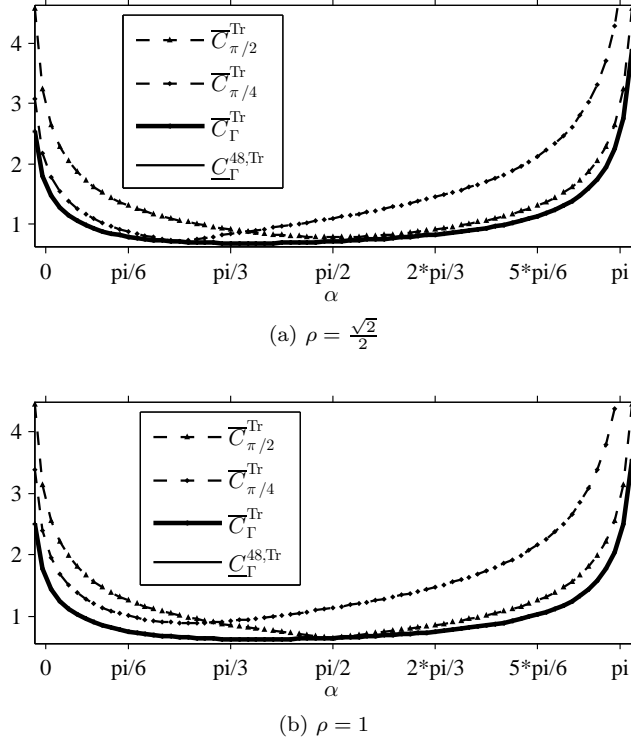
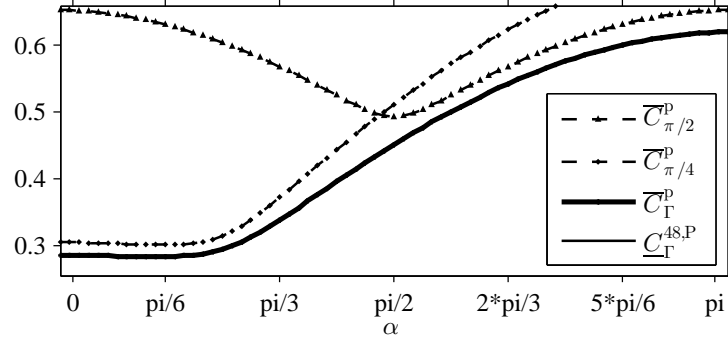
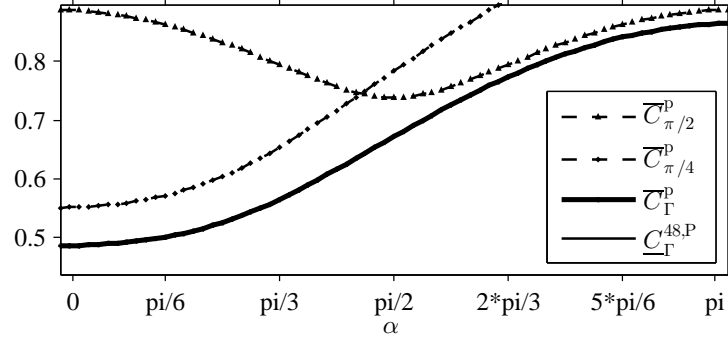


Figure 4: Lower and upper bound of  $C_\Gamma^{\text{Tr}}$  for  $T \in \mathbb{R}^2$  (a)  $\rho = \frac{\sqrt{2}}{2}$  and (b)  $\rho = 1$ .

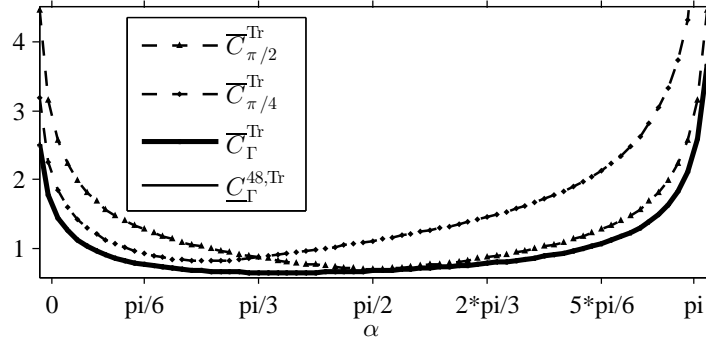


(a)  $\rho = \frac{\sqrt{3}}{2}$

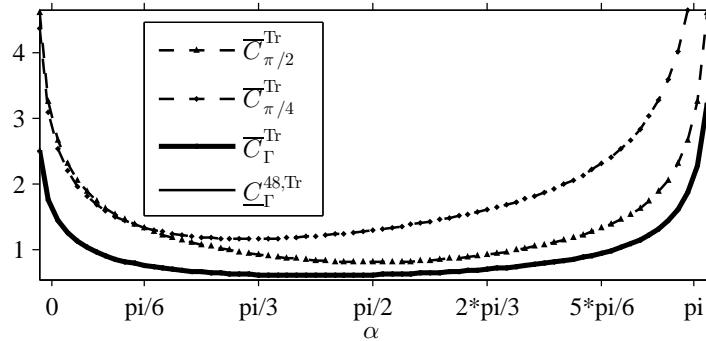


(b)  $\rho = \frac{3}{2}$

Figure 5: Lower and upper bounds of  $C_\Gamma^P$  for  $T \in \mathbb{R}^2$  (a)  $\rho = \frac{\sqrt{3}}{2}$  and (b)  $\rho = \frac{3}{2}$ .

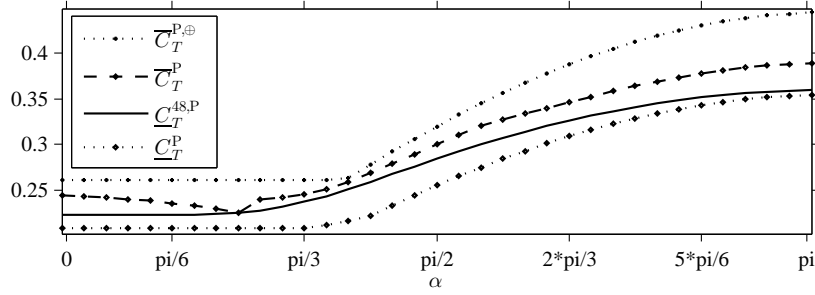


(a)  $\rho = \frac{\sqrt{3}}{2}$

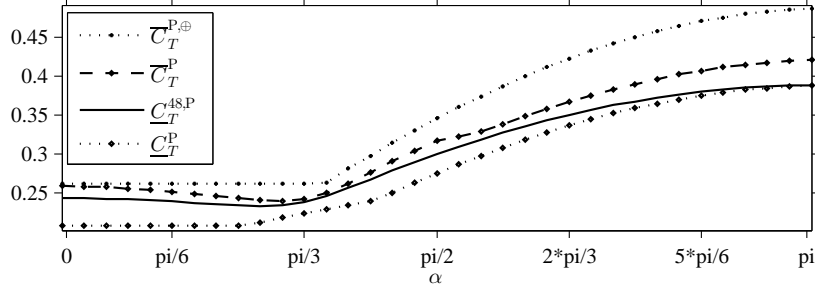


(b)  $\rho = \frac{3}{2}$

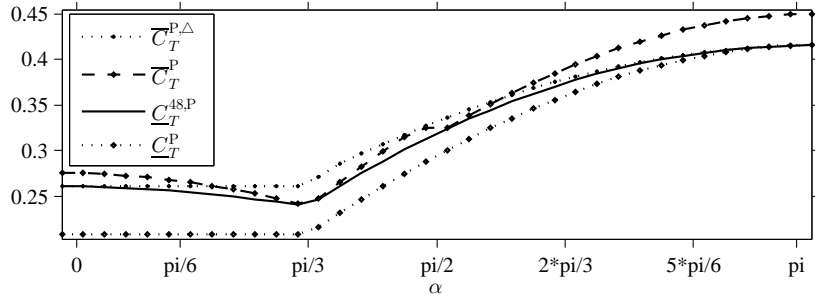
Figure 6: Lower and upper bounds of  $C_\Gamma^{\text{Tr}}$  for  $T \in \mathbb{R}^2$  (a)  $\rho = \frac{\sqrt{3}}{2}$  and (b)  $\rho = \frac{3}{2}$ .



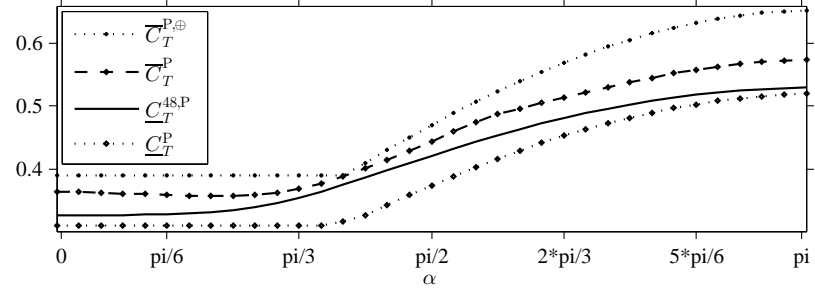
(a)  $\rho = \frac{\sqrt{2}}{2}$



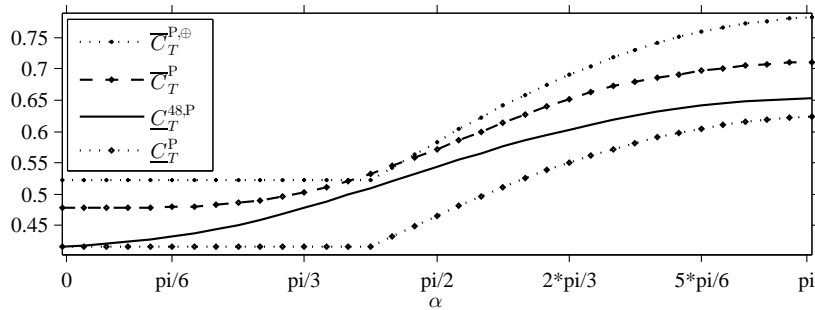
(b)  $\rho = \frac{\sqrt{3}}{2}$



(c)  $\rho = 1$



(d)  $\rho = \frac{3}{2}$



(e)  $\rho = 2$

Figure 7:  $\underline{C}_T^{48}$  with upper bounds  $\overline{C}_T^{P,\Delta}$  and  $\overline{C}_T^P$  and lower bound with respect to  $\alpha$  on  $T$  with (a)  $\rho = \frac{\sqrt{2}}{2}$ , (b)  $\frac{\sqrt{3}}{2}$ , (c) 1, (d)  $\frac{3}{2}$ , and (e) 2.

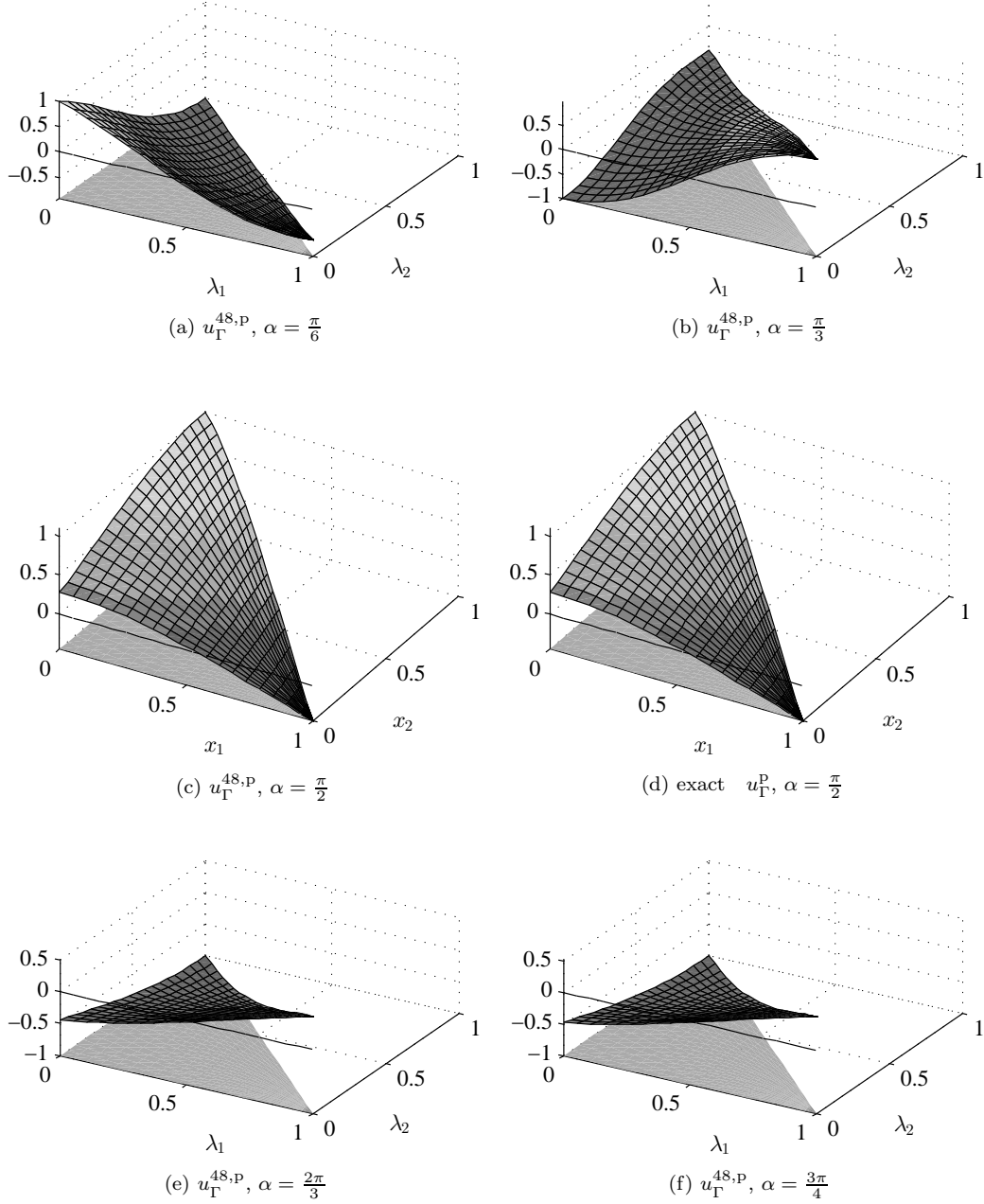


Figure 8: Eigenfunctions corresponding to  $\underline{C}_{\Gamma}^{M,P}$  and for  $M = 48$  on simplex  $T$  with  $\rho = 1$  and different  $\alpha$ .

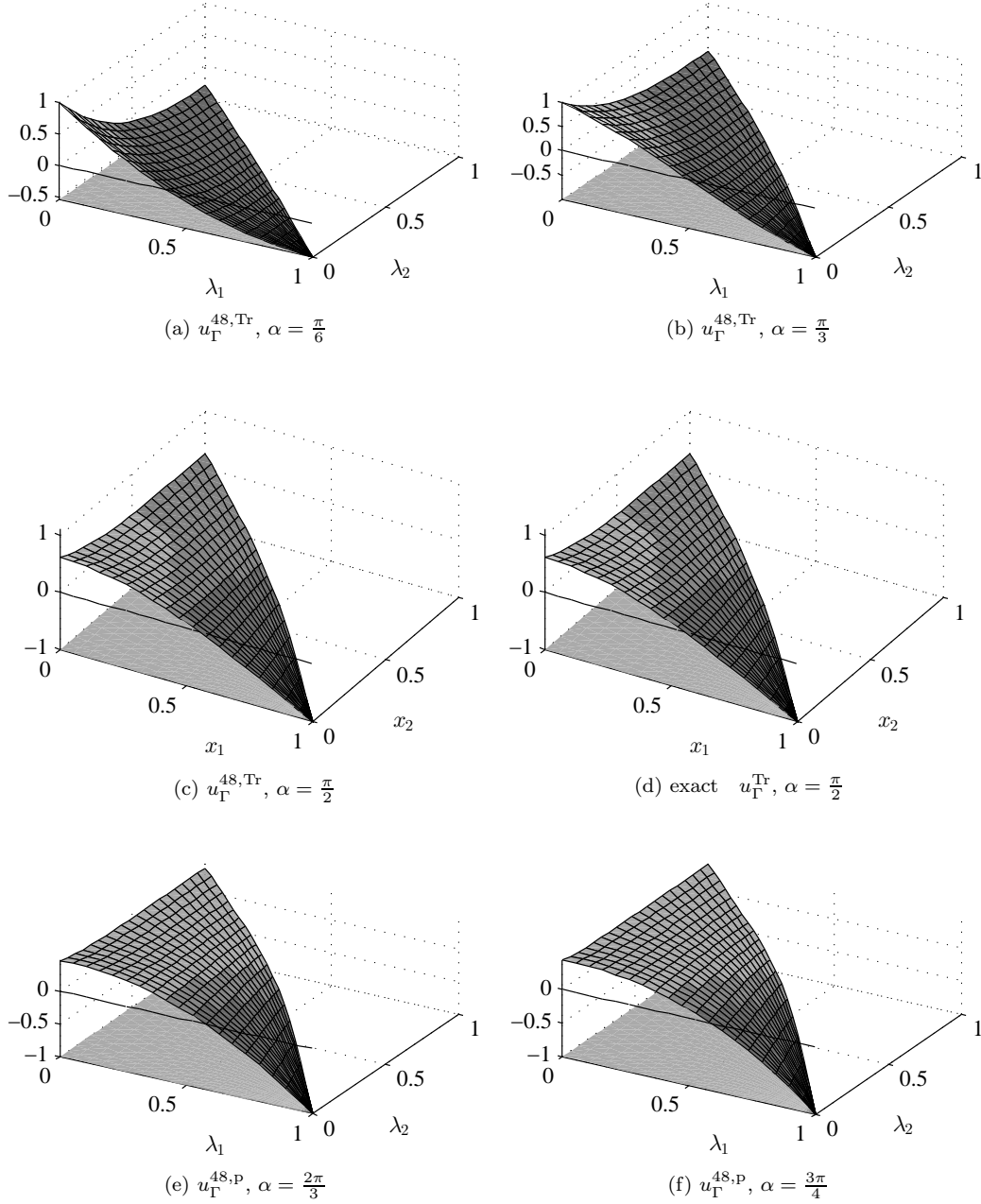


Figure 9: Eigenfunctions corresponding to  $\underline{C}_{\Gamma}^{M, \text{Tr}}$  for  $M = 48$  on simplex  $T$  with  $\rho = 1$  and different  $\alpha$ .

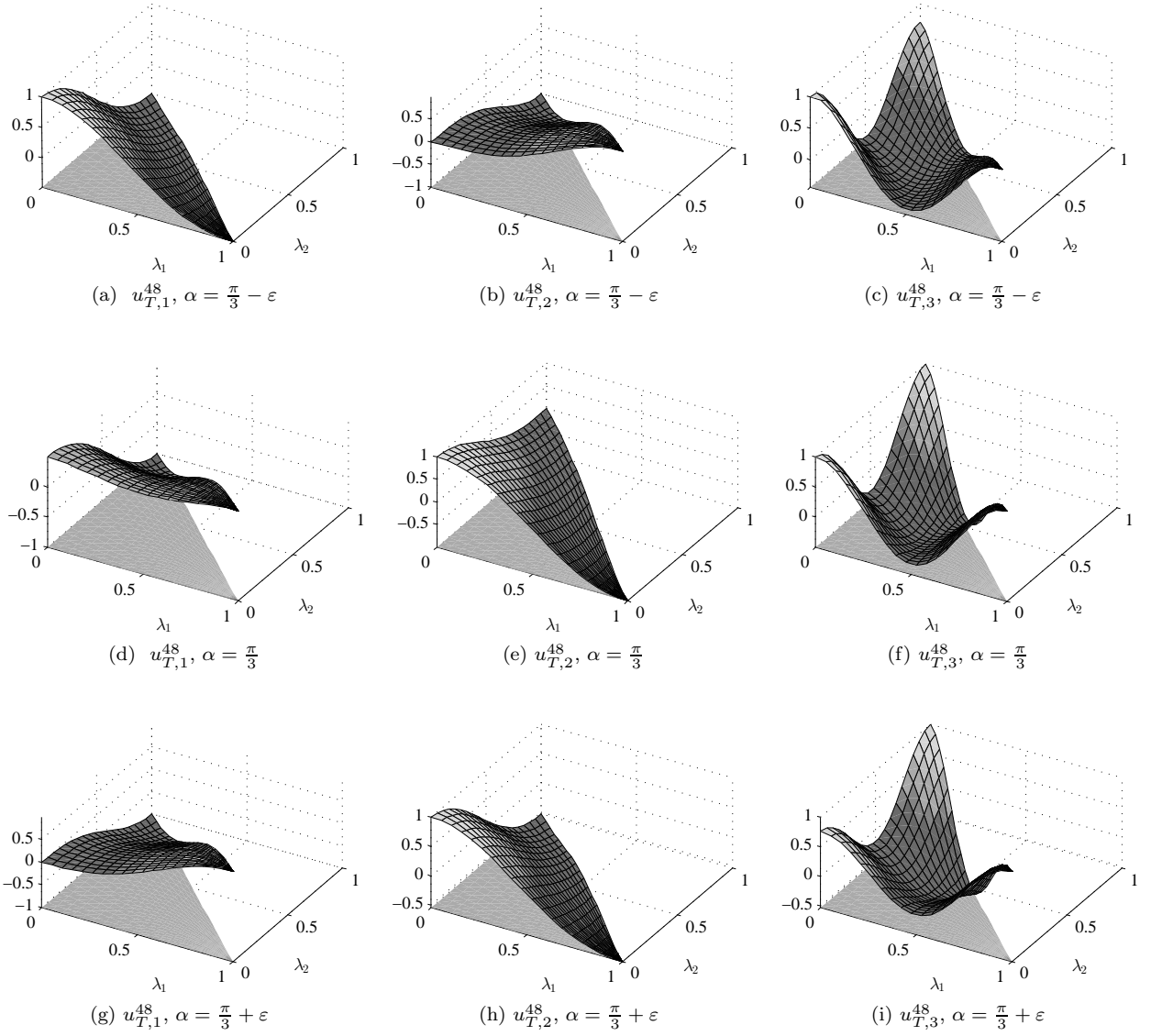


Figure 10: Eigenfunctions corresponding to  $\underline{C}_T^{M,P}$  with  $M = 48$  on isosceles triangles  $T \in \mathbb{R}^2$  with  $\alpha = \frac{\pi}{3}, \frac{\pi}{3} - \varepsilon,$  and  $\frac{\pi}{3} + \varepsilon$  in barycentric coordinates.

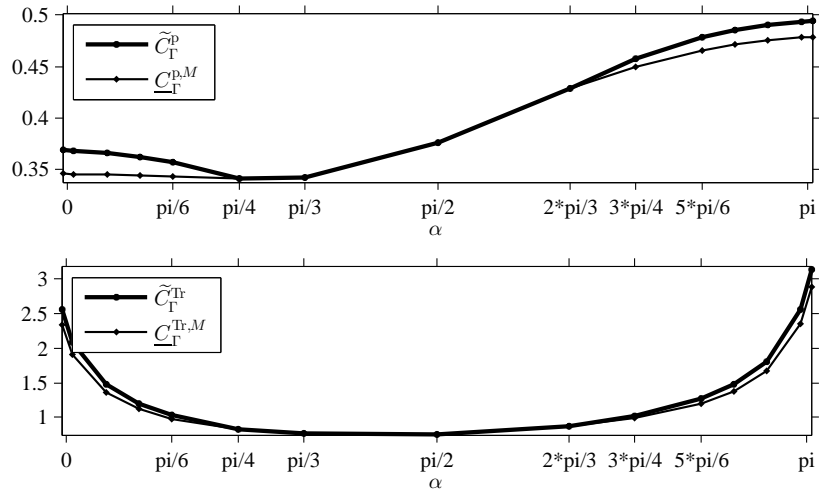


Figure 11:  $C_\Gamma^P$  and  $C_\Gamma^{Tr}$  for  $T \in \mathbb{R}^3$  with  $H = 1, \rho = 1$  with estimate based on four reference tetrahedrons.

## References

- [1] R. Bañuelos and K. Burdzy. On the “hot spots” conjecture of J. Rauch. *J. Funct. Anal.*, 164(1):1–33, 1999.
- [2] R. Bañuelos, T. Kulczycki, I. Polterovich, and B. Siudeja. Eigenvalue inequalities for mixed Steklov problems. In *Operator theory and its applications*, volume 231 of *Amer. Math. Soc. Transl. Ser. 2*, pages 19–34. Amer. Math. Soc., Providence, RI, 2010.
- [3] P. H. Bérard. Spectres et groupes cristallographiques. I. Domaines euclidiens. *Invent. Math.*, 58(2):179–199, 1980.
- [4] C. Carstensen and J. Gedicke. Guaranteed lower bounds for eigenvalues. *Math. Comp.*, 83(290):2605–2629, 2014.
- [5] C. Carstensen and S. A. Sauter. A posteriori error analysis for elliptic PDEs on domains with complicated structures. *Numer. Math.*, 96(4):691–721, 2004.
- [6] S. Y. Cheng. Eigenvalue comparison theorems and its geometric applications. *Math. Z.*, 143(3):289–297, 1975.
- [7] P. G. Ciarlet. *The finite element method for elliptic problems*. North-Holland Publishing Co., Amsterdam-New York-Oxford, 1978. Studies in Mathematics and its Applications, Vol. 4.
- [8] C. R. Dohrmann, A. Klawonn, and O. B. Widlund. Domain decomposition for less regular subdomains: overlapping Schwarz in two dimensions. *SIAM J. Numer. Anal.*, 46(4):2153–2168, 2008.
- [9] D. W. Fox and J. R. Kuttler. Sloshing frequencies. *Z. Angew. Math. Phys.*, 34(5):668–696, 1983.
- [10] M. Fuchs. Computable upper bounds for the constants in Poincaré-type inequalities for fields of bounded deformation. *Math. Methods Appl. Sci.*, 34(15):1920–1932, 2011.
- [11] A. Girouard and I. Polterovich. Spectral geometry of the steklov problem. *arXiv.org*, math/1411.6567, 2014.
- [12] Y. Hoshikawa and H. Urakawa. Affine Weyl groups and the boundary value eigenvalue problems of the Laplacian. *Interdiscip. Inform. Sci.*, 16(1):93–109, 2010.
- [13] F. Kikuchi and X. Liu. Estimation of interpolation error constants for the  $P_0$  and  $P_1$  triangular finite elements. *Comput. Methods Appl. Mech. Engrg.*, 196(37-40):3750–3758, 2007.
- [14] A. Klawonn, O. Rheinbach, and O. B. Widlund. An analysis of a FETI-DP algorithm on irregular subdomains in the plane. *SIAM J. Numer. Anal.*, 46(5):2484–2504, 2008.
- [15] V. Kozlov and N. Kuznetsov. The ice-fishing problem: the fundamental sloshing frequency versus geometry of holes. *Math. Methods Appl. Sci.*, 27(3):289–312, 2004.
- [16] V. Kozlov, N. Kuznetsov, and O. Motygin. On the two-dimensional sloshing problem. *Proc. R. Soc. Lond. Ser. A Math. Phys. Eng. Sci.*, 460(2049):2587–2603, 2004.
- [17] N. Kuznetsov, T. Kulczycki, M. Kwaśnicki, A. Nazarov, S. Poborchi, I. Polterovich, and B. Siudeja. The legacy of Vladimir Andreevich Steklov. *Notices Amer. Math. Soc.*, 61(1):9–22, 2014.
- [18] R. S. Laugesen and B. A. Siudeja. Maximizing Neumann fundamental tones of triangles. *J. Math. Phys.*, 50(11):112903, 18, 2009.
- [19] R. S. Laugesen and B. A. Siudeja. Minimizing Neumann fundamental tones of triangles: an optimal Poincaré inequality. *J. Differential Equations*, 249(1):118–135, 2010.
- [20] X. Liu and S. Oishi. Guaranteed high-precision estimation for  $P_0$  interpolation constants on triangular finite elements. *Jpn. J. Ind. Appl. Math.*, 30(3):635–652, 2013.
- [21] A. Logg, K.-A. Mardal, and G. N. Wells, editors. *Automated solution of differential equations by the finite element method*, volume 84 of *Lecture Notes in Computational Science and Engineering*. Springer, Heidelberg, 2012. The FEniCS book.
- [22] S. Matculevich, P. Neittaanmäki, and S. Repin. A posteriori error estimates for time-dependent reaction-diffusion problems based on the Payne–Weinberger inequality. *AIMS*, 35(6), 2015.

- [23] B. J. McCartin. Eigenstructure of the equilateral triangle. II. The Neumann problem. *Math. Probl. Eng.*, 8(6):517–539, 2002.
- [24] S. G. Mikhlin. *Constants in some inequalities of analysis*. A Wiley-Interscience Publication. John Wiley and Sons, Ltd., Chichester, 1986. Translated from the Russian by Reinhard Lehmann.
- [25] A. I. Nazarov and S. I. Repin. Exact constants in Poincare type inequalities for functions with zero mean boundary traces. *Mathematical Methods in the Applied Sciences*, 2014. Ppublished in arXiv.org in 2012, math/1211.2224.
- [26] D. Pauly. On Maxwell’s and Poincaré’s constants. *Discrete Contin. Dyn. Syst. Ser. S*, 8(3):607–618, 2015.
- [27] L. E. Payne and H. F. Weinberger. An optimal Poincaré inequality for convex domains. *Arch. Rational Mech. Anal.*, 5:286–292 (1960), 1960.
- [28] M. A. Pinsky. The eigenvalues of an equilateral triangle. *SIAM J. Math. Anal.*, 11(5):819–827, 1980.
- [29] H. Poincare. Sur les Equations aux Derivees Partielles de la Physique Mathematique. *Amer. J. Math.*, 12(3):211–294, 1890.
- [30] H. Poincare. Sur les Equations de la Physique Mathematique. *Rend. Circ. Mat. Palermo*, 8:57–156, 1894.
- [31] S. Repin. *A posteriori estimates for partial differential equations*, volume 4 of *Radon Series on Computational and Applied Mathematics*. Walter de Gruyter GmbH & Co. KG, Berlin, 2008.
- [32] S. Repin. Estimates of deviations from exact solutions of variational inequalities based upon payne-weinberger inequality. *J. Math. Sci. (N. Y.)*, 157(6):874–884, 2009.
- [33] Inc. ©1994-2015 The MathWorks. Mathworks. products and services, 2015.
- [34] A. Toselli and O. Widlund. *Domain decomposition methods—algorithms and theory*, volume 34 of *Springer Series in Computational Mathematics*. Springer-Verlag, Berlin, 2005.